ACS POLYMERS Au
AN OPEN ACCESS JOURNAL OF THE AMERICAN CHEMICAL SOCIETY

pubs.acs.org/polymerau

Perspective

Decoupling Ion Transport and Matrix Dynamics to Make High Performance Solid Polymer Electrolytes

Seamus D. Jones, James Bamford, Glenn H. Fredrickson, and Rachel A. Segalman*

Cite This: *ACS Polym. Au* 2022, 2, 430−448

Read Online

ACCESS | Metrics & More | Article Recommendations

ABSTRACT: Transport of ions through solid polymeric electrolytes (SPEs) involves a complicated interplay of ion solvation, ion−ion interactions, ion-polymer interactions, and free volume. Nonetheless, prevailing viewpoints on the subject promote a significantly simplified picture, likening ion transport in a polymer to that in an unstructured fluid at low solute concentrations. Although this idealized liquid transport model has been successful in guiding the design of homogeneous electrolytes, structured electrolytes provide a promising alternate route to achieve high ionic conductivity and selectivity. In this perspective, we begin by describing the physical origins of the idealized liquid transport mechanism and then proceed to examine known cases of decoupling between the matrix dynamics and ionic transport in SPEs. Specifically we discuss conditions for "decoupled" mobility that include a highly polar electrolyte environment, a percolated path of free volume elements (either through structured or unstructured channels), high ion concentrations, and labile ion-electrolyte interactions. Finally, we proceed to reflect on the potential of these mechanisms to promote multivalent ion conductivity and the need for research into the interfacial properties of solid polymer electrolytes as well as their performance at elevated potentials.

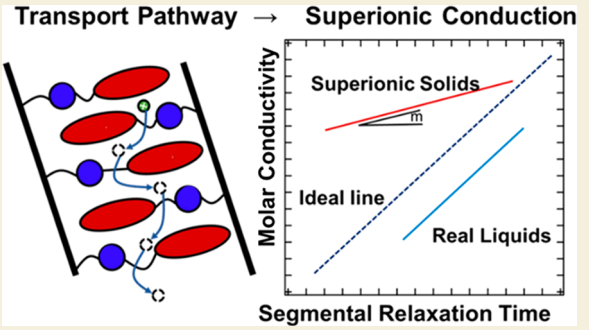

KEYWORDS: *Solid Polymer Electrolytes, Ion Transport, Superionic Conductivity, Zwitterions, Liquid Crystals, Glass Transition, Ionomers*

1. ION TRANSPORT MECHANISMS DEPEND ON THE PROPERTIES OF THE HOST MATERIAL

Ion transport is an important topic in diverse applications and materials systems ranging from simple fluids to polymers and inorganic systems. In recent decades, distinct design rules have emerged for each of these systems due to differences in their conductivity mechanisms. However, possible new innovations may emerge from cross-fertilization across material classes. Herein we describe how design principles from the polymer and inorganic electrolyte literature can be leveraged to generate polymer electrolytes with fast ion transport and selectivity (Figure 1). This section begins by describing the idealized liquid transport mechanism that is commonplace within polymer electrolytes and expands to describe deviations from this behavior that are frequently observed in structured inorganic electrolytes.

1.1. Idealized Liquid Transport Model in Polymeric Electrolytes

The operating principles of electrochemical devices require electrolytes that promote high flux of redox reactive species, typically metal cations.[1−4] Although maximizing the flux of reactive species is ultimately of primary interest for operation of high-power electrochemical devices, ion transport within an electrolyte is often parametrized by its ionic conductivity (σ), which is the transport coefficient relating the ionic current density from all charged species (i_n) to the voltage drop (ΔV) per unit distance (L) (eq 1). Nonetheless, the ionic conductivity fails to capture the complexity of engineered devices, which must have high ionic conductivity as well as high voltage stability (to operate at sufficient ΔV values) and mechanical robustness (ability to make defect-free and processable films with small L). Nonetheless, σ is a useful parameter to evaluate electrolytes as it can be easily measured using widely available impedance techniques, where more precise transport coefficients often require techniques only available to experts. Another complexity in real cells is that much of the current parametrized by the ionic conductivity may be transient conductivity that is not maintained during cell operation, since redox inactive ions will accumulate at the electrode−electrolyte interface in the absence of electrochemical reactions that can consume the charged species.[1,5]

Received: June 3, 2022
Revised: September 9, 2022
Accepted: September 9, 2022
Published: September 22, 2022

https://doi.org/10.1021/acspolymersau.2c00024
ACS Polym. Au 2022, 2, 430−448

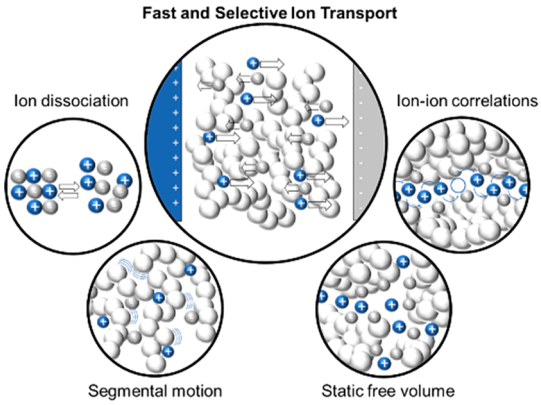

Figure 1. Polymer electrolyte performance is commonly understood to operate by the principles of ion dissociation and segmental motion. However, fundamental principles of ion conduction derived from inorganic systems such as transport through static free volume and the role of ion−ion correlations in highly concentrated electrolytes can improve efforts to engineer toward fast and selective ion transport.

Thus, full characterization of electrolyte performance for electrochemical applications must simultaneously consider the species-dependent mobilities of all mobile ions in the electrolyte or the selectivity of the electrolyte for the redox active ions, which are often metal cations such as Li^+, Mg^{2+}, or Na^+.

$$\sum_n i_n = \sigma \frac{\Delta V}{L} \tag{1}$$

Ionic conductivity is broadly governed by two interconnected factors: ion concentration and ion mobility. The mobile ion concentration is set by both the total salt concentration and the ability of the electrolyte to dissociate the relevant salt. As illustrated in Figure 2, ions within an electrolyte exist in

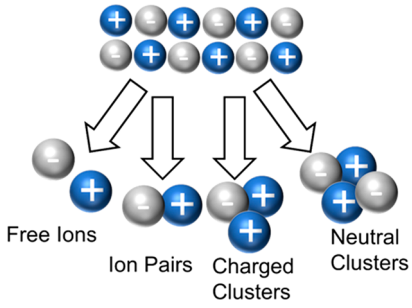

Figure 2. When a salt is introduced into an electrolyte medium it can undergo a complex equilibrium between "free" ions, associated ion pairs, and charged or neutral clusters/aggregates of >2 ions. This equilibrium plays an important role in dictating the conductive properties of an electrolyte. Similar equilibria exist for ion pairs of differing valency.

equilibrium between "free ions" (dissociated, charged ions), ion pairs (associated, neutral pairs of ions), and ionic clusters (consisting of >2 ions and may be charge neutral or charged).[6−13] When ions are associated, their motions become correlated over the lifetime of the ion association, impacting both the flux of charge and the migration of ions. Though numerous equilibria are required to describe the full population of aggregates, generally this complex equilibrium is simplified into a single equilibrium between dissociated ions and ion pairs dictated by the extent of ion dissociation (ξ) (sometimes also called the ionicity), defined in eq 2.[7,14] This dissociation extent is a function of both the identity of the ionic species as well as the properties of the background medium, including ion-electrolyte specific interactions and the overall dielectric properties of the background.[15−21]

The generation of dissociated ions generally occurs through solvation of added salts where the mobile ionic species are typically added to the electrolyte through salt-doping. In so-called single ion-conductors, which are typically comprised of a polycation or polyanion with a corresponding small-molecule counterion, the generation of mobile species occurs through dissociation of the charged polymer-small molecule ion pairs. In either case, high extents of ion dissociation (ξ) are favorable in promoting high conductivity. Since ξ can be dependent upon both the salt and the host polymer identity, it is commonly necessary to independently optimize the salt loading for each polymer/salt combination, where a typical trend of salt concentration versus conductivity displays a local maximum that is a consequence of competing effects of ion mobility and concentration.[22,23]

$$\xi = \frac{[\text{free ions}]}{[\text{total ions}]} \tag{2}$$

The ionic conductivity (σ) accounts for the net charge motion of all clusters and dissociated ions. This is seen in eq 3, where e is the elementary charge, μ_n is the specific mobility, c_n is the concentration, and z_n is the charge of cluster "n". Since neutral ion pairs do not contribute to the ionic conductivity of the electrolyte ($z_n = 0$), eq 3 only requires two terms under the simplified equilibrium of eq 2. These terms correspond to the contributions of dissociated cations and anions (eq 4), where c_{salt} is the total salt concentration. Though larger charged aggregates can also play a significant role in conductivity, especially when the salt is poorly solvated, large ion clusters have reportedly led to nonintuitive trends such as cation migration toward the cathode.[24−26]

$$\sigma = \sum_n e c_n |z_n|^2 \mu_n \tag{3}$$

$$\sigma = e c_{salt} \xi (|z_+|^2 \mu_+ + |z_-|^2 \mu_-) \tag{4}$$

In addition to generating mobile ionic species, an effective electrolyte must also facilitate the transport of these species. The standard perspective of ion motion through SPEs is derived from theories of ion transport through standard, small-molecule liquids, whereby the molecular scale (<1 nm) dynamics controls ion motion. At this length scale, the mobility of dissociated ions is primarily dictated by the local frictional environment of the liquid. The strength of the frictional force opposing ion transport is highly tied to the solvation of ions by the surrounding fluid medium.

The most widely employed theoretical treatment of the frictional coefficient is to set it as a constant proportional to the segmental relaxation time scale of the material, τ_α.[14,27,28] However, this approach fails to account for the complex specific interactions and dynamics involved. Ion motion through polymer materials does not proceed as straightforward diffusion in a liquid, but instead involves an interplay of intrachain transport, interchain hopping, and codiffusion of segments and ions.[29−37] The dynamic bond percolation or more general dynamically disordered hopping models are

https://doi.org/10.1021/acspolymersau.2c00024
ACS Polym. Au 2022, 2, 430−448

models that include consider these discrete transport processes;[33−35] these models consider ion hopping on dynamic lattices, where microscopic transport occurs through local hopping of ions on a lattice and through "renewal" events in which the lattice rearranges. Although these models do not contain molecular information, they demonstrate the importance of inter- and intrachain hopping events in ion transport. Molecular dynamics simulations have also provided information about the various ion transport mechanisms in polymer electrolytes, again finding that often multiple types of hopping events with different time scales are necessary to describe the ion dynamics of linear polymer electrolytes including inter- and intrachain hopping events as well as cluster-assisted dynamics.[31,37−41] Other hybrid approaches have provided additional theoretical backing to the complexities of determining the frictional forces applied by the electrolyte in various classes of polymer electrolyte[36,42]. Notably the number of relevant nanoscale processes further increases when the polymer is inhomogeneous or nonlinear.[43] Another complication arises from the complex free energy landscape experienced by ions.[44] The solvation of ions by the polymer not only impacts the thermodynamic equilibrium of ion dissociation but also can contribute frictional resistance to ion motion, e.g., when ions are tightly solvated by a polymer the effective friction is enhanced and ion motion suppressed.[45,46]

Although a comprehensive picture of the frictional resistance to ion motion in polymer electrolytes involves multiple relaxation time scales and chemical specificity, an ad hoc description of the diffusive behavior based on a single relaxation time has been remarkably successful in characterizing the dynamics of most polymer systems. This "Walden perspective" can be formulated for polymeric systems by arguing that the frictional force scales with the segmental relaxation time scale of the material, τ_α,[14,27,28] leading to the relation $\mu \sim \tau_\alpha^{-1}$. Data from Balsara and co-workers shows the remarkable ability of this expression to explain trends in the ionic conductivity of PEO with LiTFSI salt through direct measurements of the monomeric friction factor by quasi-elastic neutron scattering.[47] Further, researchers have utilized dielectric spectroscopy[48] and rheological measurements[20] to quantify τ_α, finding that these measured values of τ_α can describe the frictional environment of the electrolyte, even at high ionic strengths. Additionally, many authors do not have access or knowledge of these techniques and instead employ analysis of their conductivity trends based on the glass transition temperature (T_g) of the polymer as techniques to measure T_g are generally more widely available. Even this rather crude analysis of rescaling ionic conductivity by T-T_g provides a basic means to parametrize the effect of ion dynamics and can be interpreted crudely within a Walden framework as we describe below.[2,49]

Due to the coupling of ion mobility and τ_α, theories of glassy dynamics in polymers can be used to model conductivity trends in SPEs. Although the glass transition is not precisely understood in polymers, the semiphenomenological Williams-Landau-Ferry (or equivalent Vogel−Tamman−Fulcher) equation (eq 5) can be modified to model ion dynamics. Eq 5 describes the temperature-dependent dynamics of τ_α for a glass forming fluid or polymer. By substituting this expression for mobility into eq 4, we obtain eq 6, which provides a proportionality expression for the molar ionic conductivity (Λ, $\Lambda \equiv \sigma/c_{salt}$) as a function of temperature. This may be calibrated using the ionic conductivity of a dilute reference system to obtain values for A, which depends on the salt identity and relates to the frictional coefficient exerted by the medium. Although this simple treatment of the friction coefficient imposed by the electrolyte is not rigorous for many electrolytes (as discussed above), this analysis can be used as an idealized reference. Although this elegant means of relating the temperature-dependent ion dynamics to the glass transition is established, it is commonplace within the field of SPEs to instead treat all constants within the WLF equation as totally phenomenological, thus omitting any possibility to make a fundamental connection between the polymer dynamics and the glass transition.

$$\mu^{-1} \sim \tau_\alpha = \tau_\alpha(T = T_g) \times 10^{-C_{1g}\times(T-T_g)/C_{2g}+T-T_g} \tag{5}$$

$$\Lambda = \frac{\sigma}{c_{salt}} = \xi A[\tau_\alpha(T = T_g)]^{-1} \times 10^{C_{1g}\times(T-T_g)/C_{2g}+T-T_g} \tag{6}$$

The coupling of ion dynamics to the glass transition presents a conundrum for designers of amorphous SPEs. Typically, molar conductivities on the order of ∼1 S cm^2/mol are required to provide a viable replacement to liquid electrolytes. Consequently, a segmental relaxation time of $\tau_\alpha \sim 10^{-9}$ s is required, suggesting that idealized liquid transport of SPEs can only provide sufficient ionic conductivities at temperatures ∼90 °C above their glass transition temperatures (if typical values of C_{1g} = 17.44 and C_{2g} = 51.6 K are used). Although it is possible to design sufficiently low-Tg polymers to achieve this temperature window, balancing the low T_g as well as other requirements of an electrolyte presents a major challenge, particularly since mechanical robustness is generally a major justification for choosing a polymer over a liquid electrolyte. Furthermore, the idealized liquid transport mechanism generally results in poor selectivity for ions of interest relative to other ions in the system.

The selectivity of the electrolyte in the fully dissociated limit is a consequence of the unequal diffusion of the cations and anions of the system. The cation transport number, t_+, is computed according to the self-diffusion coefficients of all mobile ionic species/clusters in the electrolyte (shown in eq 7 for the simplified equilibrium of eq 2). Although eq 7 is subject to the same approximations as the previous expression and has the same limitations as a descriptor for a real system, this expression demonstrates the principle that selectivity is difficult to attain in an idealized liquid transport mechanism since both $\tau_\alpha^{-1} \sim \mu_+$ and $\tau_\alpha^{-1} \sim \mu_-$, suggesting limited dependence of selectivity on the design of the electrolyte. Balsara and co-workers also observe significant challenges imparting selectivity in polymer electrolytes, where an increase in selectivity across many electrolytes is accompanied by a dramatic reduction in conductivity.[1] These challenges further motivate the design of systems where ion dynamics and segmental dynamics are decoupled since alternative modes of conduction (such as those displayed in inorganic electrolytes) typically display much greater selectivity for cations of interest.

$$t_+ = \frac{|z_+|^2\mu_+}{|z_+|^2\mu_+ + |z_-|^2\mu_-} \tag{7}$$

1.2. Amorphous SPE Designs

Standard strategies toward improving SPE conductivity primarily rely either on improving the solubility of salts within

https://doi.org/10.1021/acspolymersau.2c00024
ACS Polym. Au 2022, 2, 430−448

the electrolyte (increasing ξc_{salt}) or increasing the mobility of salts by reducing the glass transition temperature of the electrolyte. Linear poly(ethylene oxide) (PEO) has become a model polymer host for lithium conduction as the coordination of ether-oxygens with lithium has been shown to yield high solubilities of lithium salts such as lithium bis-(trifluoromethanesulfonyl)imide (LiTFSI) or lithium hexafluorophosphate ($LiPF_6$) and the relatively low T_g of the polymer promotes ion mobility via the idealized liquid conduction mechanism.[3,50] These properties have made PEO the most highly studied SPE host despite its relatively poor mechanical and selectivity properties. Although PEO is a semicrystalline polymer, its conductivity in the amorphous state is of primary relevance for most applications since the ionic conductivity in this state is typically much higher than below the melting temperature,[51,52] except in exceptional cases.[53] Many detailed reports have investigated the transport mechanism for this polymer,[47,54,55] finding it to mainly display idealized liquid transport at low salt compositions and above its melting temperature.

Although amorphous PEO is known to generally follow an idealized liquid mechanism, several factors can result nonideal conductivity trends. This suggests that conductivity in these systems may also depend on solvation site dynamics and percolation. For example, Hawker and co-workers studied the impact of PEO-based materials with linear and cyclic ether side chains, finding that the ionic conductivity of the linear and cyclic polyethers were similar despite significant differences between the glass transition temperatures of these two polymers.[56] Similarly, work by Patel and co-workers has experimentally and theoretically studied side-chain polyethers; they found that ionic conductivity differences between linear and side-chain polyethers of differing lengths are not explained by differences in segmental mobility of the system.[43,57] The conductivity trends of these systems were attributed to differences in solvation site connectivity and the dynamics of these sites, which were found to differ depending on the distance of the chelating groups from the backbone.

Attempts to improve the performance of PEO primarily focus on reducing its crystallinity, further reducing the T_g, and improving its salt solvation ability. The crystallinity of PEO can be reduced by designing nonlinear architectures,[43,56−58] addition of additives that inhibit crystallization,[59−61] cross-linking,[62−64] and using copolymerization to reduce the ordering of the PEO.[65,66] Small molecule additives can play various roles including as plasticizers[67−69] and dielectricizers.[70,71] In general, PEO is poorly selective ($t_+ < 0.2$), and the addition of anion traps can modestly increase selectively.[72−75] A variety of other amorphous hosts based on other coordinating groups have also been reported; however, none of these candidates reliably surpass the benchmarks set by PEO.[50,76] Indeed, it appears in most cases that as conductivity is increased, selectivity is sacrificed resulting in a practical upper bound in performance.[1]

1.3. Superionic Ceramics Support Different Transport Mechanisms

While our discussion of SPE conductivity up to this point has focused on the idealized liquid mechanism of transport, where ion transport is coupled to fluid relaxation, some materials display relatively fast transport of ions despite having slow relaxation dynamics. Diverse materials ranging from carefully designed ceramics[77] to ice at extreme pressure and temperature conditions[78,79] can display high decoupling of ion transport from their matrix motion. Mechanisms for charge transport in these solid systems do not involve translational diffusive motion of the electrolyte since the atomic coordinates of crystalline or amorphous ceramics are strongly confined by steep energy wells, yet high ionic conductivities above 10^{-2} S/cm have been reported.[80] So-called superionic transport in inorganic electrolytes relies upon immobile percolated pathways of free volume, allowing ions to opportunistically hop along a pathway of sites comprising vacancies, interstitials, or voids at rates that can exceed those attainable in simple or polymeric fluids. Moreover, the fixed nature of the sites enables great size-based selectivity of ion transport in these electrolytes (often approaching $t_+ = 1$ for lithium salt systems).[80,81]

Ion transport decoupled from matrix motion has been demonstrated in many ceramic materials, which are often crystalline in nature, and yet, display ionic conductivities on par with simple fluids. Extensive work detailing the design of these materials is already published,[82−89] so here we summarize some key findings from this field that may be applicable to SPEs. First, it is known that a percolating network of free volume sites must be present to promote sufficiently rapid ionic motion. In these cases, the energy to hop between sites is often conceptualized to follow an Arrhenius-type process where energy for an ion jump process in isolation is controlled by factors such as the local free volume and the interactions between the ion and the matrix. These two features require that the equilibrium packing of the electrolyte be loosely spaced to accommodate the mobile ion and that the chemical properties of the matrix are sufficiently labile such that ions can dissociate from their local interactions to allow for fast hopping rates. This resembles the solvation strength trade-offs which can be present in SPEs and prevent the activated hopping of ions between sites in these materials. Another relevant feature is the collective nature of motions in these types of materials (Figure 3, adapted from ref 89). It has been shown that a significant amount of the transport is due to 'stringlike motions' where the presence of nearby ions can lower the energy barrier for ion transport in these materials. This type of mechanism can only occur at sufficiently high ion loadings, and ion concentrations in these materials typically exceed levels seen in polymer or liquid electrolytes.

Another crucial design principle is the requirement of mobility within superionic crystals. In both inorganic glasses[90] and crystalline inorganic solids,[91] crankshaft-like motions of the matrix are crucial in driving the motion of lithium; this effect is often called the "paddlewheel" effect.[90,91] These types of microscopic motion typically consist of rotation and vibrational modes and thus do not truly correspond to rearrangement of the crystal but nonetheless can set temperature floors for operation of ceramic crystals and devices. These motions arise below the melting temperature of the material; phenomenologically it has been observed that they can arise at $T \sim 2/3T_m$.[83] Although ion transport is often still temperature-dependent in these electrolytes, phonon-assisted transport in rigid ceramics is typically much less temperature sensitive than in glass-forming liquids, allowing excellent ion transport performance over a range of temperatures.

Another remarkable aspect of ceramic ion conductors is their near-universal high selectivity for ions of interest in many applications. Indeed, in lithium-conducting ceramics the transport number of lithium often approaches unity, suggesting almost complete exclusion of counterion motion.[92] This is

https://doi.org/10.1021/acspolymersau.2c00024
ACS Polym. Au 2022, 2, 430−448

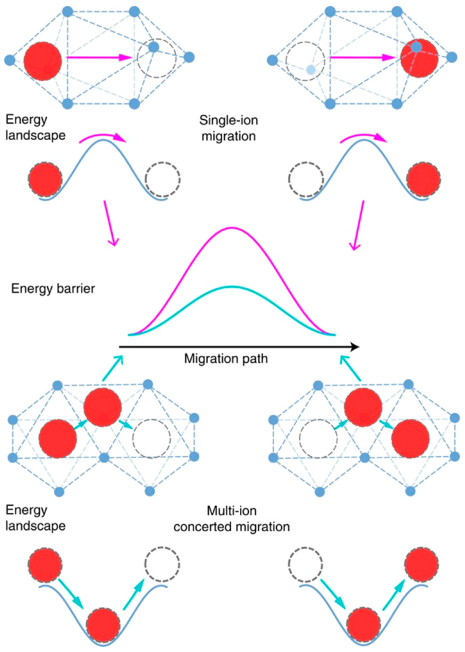

Figure 3. Transport pathways in superionic ceramics can be dominated by cooperative hopping events. In the case of a discrete ion (pink), the ion experiences a larger energy barrier for hopping than in the case of the cooperative event (green) where the correlation of the ion motions results in a lower overall energy barrier that these ions must overcome. Reprinted with permission under a Creative Commons CC BY License from ref 89. Copyright 2017 Nature Publishing Group.

attained based on the precise size-selectivity of these structures. Since alkali metal ions such as lithium are typically much smaller than their counterions, the size selective nature of these structures can prevent counterion motion altogether, leading to t_+ approaching unity.

Although the design principles of ceramic materials are inarguably different than SPEs, some design principles from such systems are likely to be maintained. The free-volume pathway for ion motion is likely to be a necessary design feature of either class of material. This free volume pathway can be realized in ordered crystalline solids, fragile glasses, or through nanoscale ordering of soft materials. Additionally, it is seen that ion−ion correlations between mobile ions can play a positive role in promoting the concerted motions of ions. This type of motion is likely to be rarely implemented in organic polymeric electrolytes since common ion loadings are too low; however, in systems like polymer-in-salt electrolytes these concerted motions may play a larger role. Finally, the ion solvation of SPEs can be a great concern. Attaining high salt loadings is crucial to leverage superionic effects, but it can be challenging to simultaneously impart high solubility while maintaining labile electrolyte-ion interactions.[16,93]

1.4. Analysis of Transport Mechanisms

Although the assignment of transport mechanism to material class is trivial in some cases, for instance, in fluids well above their melting or glass transition temperature, an idealized liquid mechanism is almost universally responsible for transport, some materials such as polymers represent a more complicated case where the dominant mechanism of transport may be system-dependent and nonintuitive. Walden plot analysis[27,28,94] is a tool used to evaluate the transport mechanism. This construct evaluates the transport rate in comparison to the measured rate of fluid relaxation, allowing comparison between experimental results and a ideal liquid Stokes−Einstein perspective of transport. The shape of the curve in the Walden construction can assist in identifying the transport mechanism and can reveal the role of ion aggregation, making it a useful experimental tool for practical analysis of ion transport; however, due to its simplified nature, it should be employed along with theory and structural characterization, particularly for complicated materials.

Walden plot analysis compares the average mobility of the ionic species within an electrolyte to the anticipated ionic mobility based on the idealized liquid transport mechanism. Figure 4 shows a representative Walden plot,[14,27,28,94] where

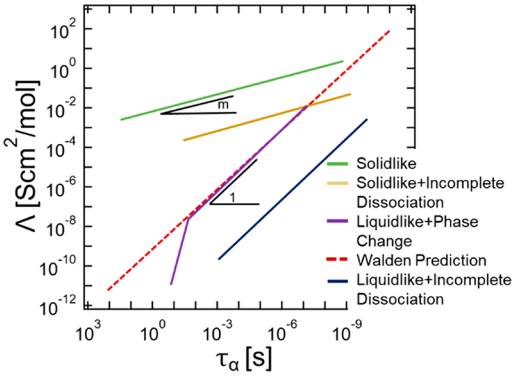

Figure 4. This figure shows a representative Walden plot where the red dashed line shows the Walden prediction line applicable to most ideal liquid electrolytes. The blue line is a fluid with partial ion aggregation resulting in suppressed ionic conductivity. The green line is superionic material with decoupled transport. The yellow line is a superionic material with partial ion aggregation, and the purple line represents a material undergoing a crystallization transition. The slope "m" < 1 represents decoupling of matrix dynamics and ion transport.

the red line indicates the Walden prediction that is dictated by the scaling relation $\Lambda \sim \tau_\alpha^{-1}$, and the absolute magnitude of the line is calibrated based on the conductivity of an ideal dilute solution. This line is typical of a simple fluid with $\xi = 1$ (complete salt dissociation) and represents complete coupling of segmental motion of the polymer matrix to ionic transport. This line is the Walden prediction, and it separates the region of subionic (slower than ideal liquid transport rates) and superionic behavior (faster than ideal liquid transport rates). Agreement between measured data and the Walden relation may indicate systems that proceed ideally by the idealized liquid transport mechanism and with full dissociation of ions. This behavior is typical in dilute solutions of salts in small molecule fluids and in polyether electrolytes at low salt concentrations, though it is known that ion transport behavior in polyethers actually can be more complex than this simplified picture.

Departures from ideal Walden behavior may be highly informative in indicating the transport physics of a system. One common source of departure from this line may come from incomplete ion dissociation, i.e., $\xi < 1$[7]. This case is highlighted by the blue line and commonly arises in ionic liquids or concentrated electrolytes. The line still is parallel to the Walden line with $\Lambda \sim \tau_\alpha^{-1}$; however, the ionic conductivity is reduced compared to this line due to a fraction of electrochemically inactive, charge-neutral species. In simple

https://doi.org/10.1021/acspolymersau.2c00024
ACS Polym. Au 2022, 2, 430−448

fluids, this deviation can often be described by the Haven ratio (H), which is defined as the ratio of tracer diffusion (D_t) to charge diffusion (D_σ) ($H = D_t/D_\sigma$), where D_t is frequently determined from solid-state NMR measurements.[95] This quantity may reflect effects of ion-pairing, ion cluster formation, and other charge−charge correlations. Additional information regarding ion correlations can be gleaned from NMR measurements of the electrophoretic ion mobilities;[96] however, relatively few studies have been published to date.

Departures from ideal Walden behavior may also indicate a nonideal transport mechanism. The green line represents another strong deviation from the Walden line typical of superionic ceramics and certain inorganic glasses. The value of this "m" parameter is called the decoupling index and often ranges from zero to unity, where m values approaching zero represent complete decoupling of ionic transport from matrix motion, and a decoupling exponent of unity represents completely coupled ion and matrix motion. Voronel[28] has shown that m values for typical fluids fall from 0.8 to 1, suggesting only slight decoupling of ion and matrix transport. Values of m can also exceed unity in some rare cases. This may arise from a thermodynamic phase change such as seen during the crystallization of PEO (represented by the purple curve). It is also reported in some inhomogeneous fluids with multiple time scales for dynamics, where the origin of $m > 1$ appears to arise due to dispersed "vacancy regions" that display faster dynamics than the surrounding fluid, leading to a breakdown of the fractional Stokes−Einstein relationship.[97−99] In some cases, both effects of incomplete salt dissociation and breakdown of Stokes−Einstein dynamics may occur,[100] resulting in behavior where both superionic and subionic behavior occur in the same system as represented by the yellow line. Additionally, thermodynamic transitions such as crystallization can impact the ion conduction mechanism. The purple line is representative of PEO, which typically follows the Walden relation above T_m but becomes subionic upon crystallization.

Utilizing the Walden plot requires accurate measurement of both the molar conductivity of the ions in the electrolyte as well as τ_α. Most frequently the ionic conductivity determined from dielectric spectroscopy is used along with the known ion concentration to determine the molar conductivity, although this can lead to complications in cases of incomplete ion dissociation since a portion of the ions will not contribute to the measured ionic conductivity. This may be corrected by renormalizing the conductivity to reflect the concentration of dissociated ions in cases where the ion dissociation extent can be determined. Alternatively, it is possible to utilize direct measurements of ion diffusion coefficients from NMR-based measurements.[101,102] In this case, the Nernst−Einstein relation may be used to convert the Walden prediction to a prediction of diffusivity. Although the framing of the Walden relation is classically formulated as a prediction of the molar conductivity, it may be more fundamentally useful to frame this relation in terms of a diffusivity axis or to renormalize based on the fraction of dissociated ions.[100]

The determination of the segmental time requires grappling with the complex nature of fluid relaxation, especially near the glass transition temperature. Experimentally the segmental relaxation may be determined via a variety of means including scattering techniques,[23,103−105] broadband dielectric spectroscopy,[23,106] rheology,[20,106] and NMR;[107,108] however, these techniques are specialized and are often not reported for SPEs. In a recent review, Sokolov proposes that the experimentally measured glass transition temperature,[2] which is much more standardized in its measurement, may provide a crude means to estimate glassy dynamics in the literature using the relation $\tau_\alpha(T = T_{g,\text{calorimetric}}) \approx 100$ s. This expression provides a single point to compare dynamics; however, polymers cannot be placed on a Walden plot using this information unless the variation of dynamics with temperature is known. Extrapolation based on the "universal" form of the WLF equation is in principle a means to tackle this issue. However, such an approach suffers from difficulties in fitting the universal function.[109] Computationally, the measurement of glassy dynamics also comes with its own challenges. While atomistic molecular dynamics simulations can access picosecond to microsecond relaxation phenomena, this time scale range is still insufficient to capture matrix dynamics relevant for the calorimetric glass transition, which involves geologically relevant time scales.[98,110] Furthermore, glass formation behavior is dynamically heterogeneous, wherein the relaxation is highly spatially dependent. This dynamic heterogeneity may cause additional issues when collecting particle-by-particle statistics as a larger ensemble of particles may be necessary to capture the average behavior.

2. LEVERAGING ALTERNATIVE ION CONDUCTION MECHANISMS

A limited but growing number of polymeric systems have been demonstrated to have deviation from liquidlike transport, some with superionic transport akin to ceramics, as described below.

2.1. Highly Polar Zwitterionic Electrolytes Solvate High Salt Concentrations

Crystalline zwitterionic (ZI) compounds with bulky and diffuse ion groups show great promise as solid-state ion conductors due to their charge neutrality, excellent dielectric properties, and unique self-assembly behaviors. ZIs are comprised of an anion and cation that are connected by a short tether, typically an alkyl spacer 3−4 carbons long. Due to this covalent ion attachment, ZIs are charge-neutral molecules with extreme values of the dielectric constant, dielectric constants as high as 270 have been reported in the amorphous state.[111] These properties make for useful ion transport hosts as the charge-neutral ZI will not migrate in an electric field but can act as a highly polar background to promote ion transport of ions when blended with salt.[111,112] Indeed, the excellent dielectric properties of ZIs promote ultrahigh salt solubilities without ion pair formation, even up to equimolar salt/ZI loadings.[111,113] Furthermore, ZIs display a broad range of ordering motifs (e.g., fluid, liquid crystal, and crystal) due to the strong intermolecular interactions among the charged groups. Interestingly, zwitterions display significantly more ordering than their ionic liquid counterparts even when they are comprised of the same ionic components, with significantly wider windows of stability for the crystalline phase and higher melting temperatures.

Some polymeric zwitterions display superionic transport of ions without the disadvantages of purely polycrystalline electrolytes such as poor contact with electrodes,[114] brittleness and cracking,[115,116] and limited chemical/electrochemical stability against a metal anode or high-energy cathode[117]. Semicrystalline materials can mitigate some of these disadvantages; for instance, they display superior contact with electrodes via amorphous domains (which can mitigate the

https://doi.org/10.1021/acspolymersau.2c00024
ACS Polym. Au 2022, 2, 430−448

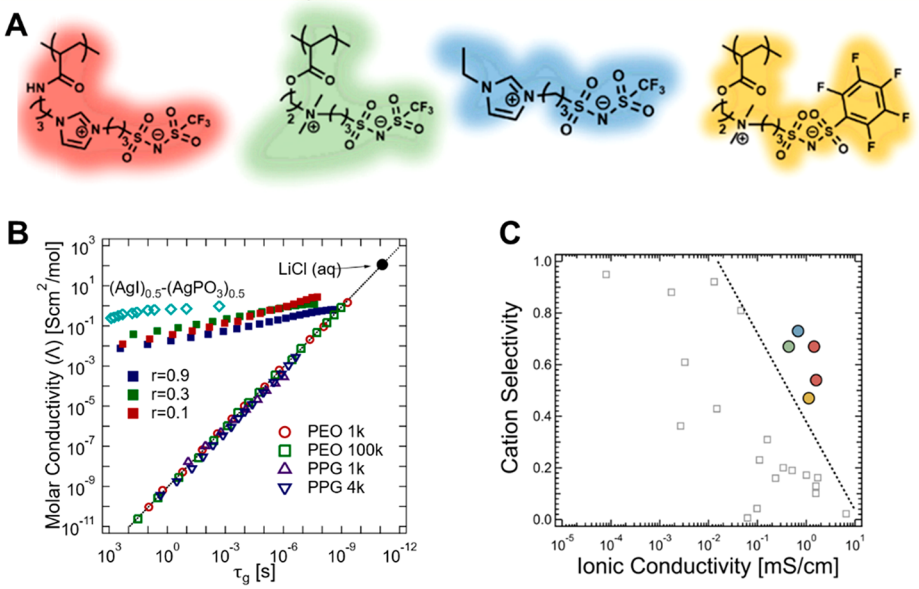

Figure 5. (A) ZI polymers (red, green, and yellow) and ZI-small molecule (blue) that were studied as Li^+ electrolytes in our previous work. (B) A Walden plot analysis of the red-highlighted ZI polymers at various salt loadings (r = moles of LiTFSI salt/mol of ZI) shows strongly superionic behavior of the ZI polymers.[119] ZI Polymer behavior is nearly competitive with superionic ceramic materials in terms of decoupling from the ideal liquid conduction mechanism (inspired by Sokolov and co-workers[27]). (C) Analysis of ZI polymer conductivity and selectivity performance surpasses a phenomenological "upper-bound" for SPE performance as proposed by Balsara and co-workers[1] (colors of the points correspond to the zwitterionic structures in panel (A), uncolored points are literature data from Balsara and co-workers). Adapted with permission from ref 119. Copyright 2022 American Chemical Society.

presence of a resistive electrode−electrolyte boundary). Additionally, they can display superior mechanical properties and processability since the amorphous portion gives ductility, and the crystalline portions provide rigidity against deformation. The advantages of semicrystalline electrolytes are discussed in greater detail by Mauro and co-workers.[118] Our recent work studied a ZI (Figure 5A), and ZIs tethered to linear polymer chains such that the cation of the zwitterion was connected to each monomer.[119,120] We used Walden plot analysis to show that these polymers displayed transport behavior strongly decoupled from the segmental relaxation behavior (Figure 5B), similar to a solid silver iodide/silver phosphate glass. This decoupling suggests a structural motif that enables superionic behavior. The polymers were analyzed by calorimetry and X-ray scattering and found to be semicrystalline, possessing structural similarity between the polymeric zwitterion (PZI) and the equivalent crystalline ZI. We believe that a similar hopping-type transport mechanism may be present in both the polymeric and nonpolymeric versions of this zwitterion, accounting for the observed superionic transport behavior. This transport mechanism leads to an excellent balance of conductivity and selectivity when analyzed against literature results compiled by Balsara and co-workers[1] (Figure 5C).

The excellent performance of polymeric zwitterions as solid and Li^+ selective hosts for ion transport has inspired further investigation of these compounds. Both small-molecule and polymeric ZIs surpass a phenomenological upper-bound proposed by Balsara and co-workers[1] when analyzed in terms of their selectivity and transport properties. This suggests the excellent promise of these semicrystalline electrolytes as ion transport materials. In recent work, we have further elucidated structure−property relationships for these materials, finding that the bulkiness (ion volume) of the tethered ions closely correlates with the ionic conductivity of the electrolyte. This is consistent with common notions in ionic liquid literature which suggests that more diffuse ions often display more labile ion−ion interactions and faster ion transport. This suggests that both the nanoscale ordering of the zwitterion as well as the strength of zwitterion-salt interactions are crucial in promoting efficient ion transport in ZI materials. In the proceeding text we further review work on ZI electrolyte materials, focusing on recent work that characterizes the simpler case of small-molecule ZIs.

As in ceramic materials, the structure of ZIs is hypothesized to intimately relate to their ion transport properties and mechanism, suggesting the importance of understanding zwitterion phase behavior. Though ZIs and ionic liquids are composed of the same ions, distinct differences arise in the phase behavior of ZIs due to the tethered nature of these ions. For instance, while imidazolium and sulfonamide ions constitute some of the most common room temperature IL's such as 1-ethyl-3-methylimidazolium bis-(trifluoromethylsulfonyl)imide (T_m = −16 °C), when they are joined together by a relatively short tether, they form a ZI with a relatively high melting point (T_m = 131 °C[121]). The structure of ZI/salt blends is particularly important in electrolyte applications as the addition of salt is required to generate charge carriers for the electrolyte. Ohno has observed that the addition of equimolar salt to a crystalline ZI results in the disappearance of a crystalline melting peak and the appearance of a glass transition when analyzed in calorimetry,[121] suggesting an amorphous structure of ZI/salt blends at high salt loadings. This is studied in greater detail by Pringle and co-workers, who have found crystalline phases at both the high and low salt concentration extrema and a liquid phase at intermediate composition.[122] We have investigated the composition-dependent phase behavior of zwitterion-salt

https://doi.org/10.1021/acspolymersau.2c00024
ACS Polym. Au 2022, 2, 430−448

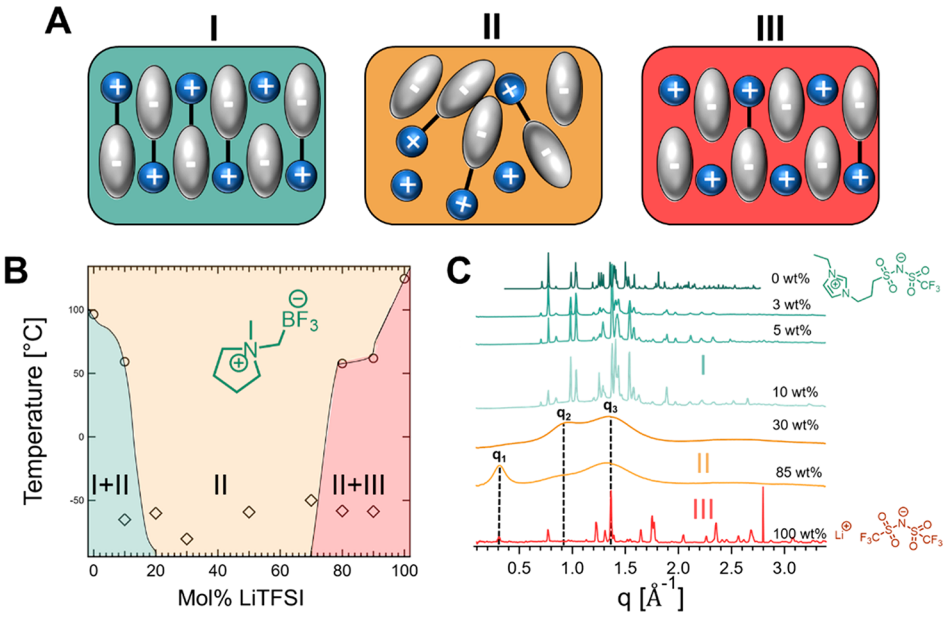

Figure 6. A)The three regimes of zwitterion behavior that seem apparent include (I) a zwitterionic crystal regime (II) a liquid consisting of zwitterion and salt, and (III) a salt crystal regime. (B) Pringle and co-workers measured the calorimetry of a zwitterion/salt blend.[122] Based on their measurements, a preliminary phase diagram can be prepared; this diagram has coexistence regimes at both extrema and a large liquid window in the center of the phase diagram. (C) Blends of a zwitterion consisting of IL-like ion pairs is found to display solidlike behavior at low salt concentrations indicated by sharp Bragg peaks. Then at intermediate salt loadings, the Bragg peaks give way to liquidlike structuring with an ion−ion correlation peak (q_2) and a liquidlike packing peak (q_3). At higher salt loadings, the presence of a third peak q_1 that likely corresponds to salt aggregates emerges.

mixtures, suggesting eutectic-like behavior at intermediate compositions that is heavily dependent upon both the structure of the zwitterion and the added salt identity, with bulkier salts generally being more disruptive to the crystallization of the zwitterionic electrolyte. Zwitterion/salt blends studied in the literature appear to universally behave as eutectic mixtures with three major structural motifs: (Figure 6A) (I) a zwitterion-rich crystalline regime that exists at low salt concentrations, (II) a disordered liquid regime that exists at intermediate concentrations of salt and zwitterion, and (III) a salt-rich crystalline phase that contains some zwitterion. In the following, we will discuss the structure and ion conduction properties within each regime.

At low concentrations of salt, the ZI retains its crystalline nature and displaying nonideal transport properties. Pringle and co-workers studied a pyrrolidiunium/boron trifluoride ZI (Figure 6B inset structure) in the presence of lithium/TFSI salt. They found (Figure 6B) a T_m (indicating motif I) and a T_g (indicating motif II) at 10 mol % salt loading. This suggests a coexistence of ZI crystals (motif I) with a disordered fluid (motif II) that is present at appreciable salt concentrations. Similarly, we studied the structure of blends of Li/TFSI salt and ZIs comprised of ethyl-imidazolium/TFSI ion pairs with a propyl spacer between the ions (Figure 6C). We also found that 10 wt % salt blends maintain Bragg reflections that coincide with the Bragg reflections of the pure crystal, again suggesting coexistence of crystal (motif I) and liquid regions (motif II). Another universal feature of both blends is the reduction of the melting temperature as salt is added. Pringle and co-workers observe a T_m reduction of ∼40 °C at 10% salt where we see a similar reduction of about 60 °C at a similar salt composition. This reduction is typical of eutectic mixtures and is commonly observed in metallurgical systems where it can suggest the formation of "alloys" where two components are cocrystallized together into one structure. More work is required to understand the thermodynamics of zwitterions and whether similar alloys can form, as this alloying may have profound implications on the ionic transport of these structures. The melting temperature of these ZI/salt blends may also play an important role. While low melting temperatures can be associated with faster ion transport as implied by the Tamman rule, which suggests a coupling between transport and T_m within a crystal, melting within the operational window of the electrolyte can cause issues such as electrolyte leakage or fracture of the electrodes on recrystallization. These issues may lead to reduced utility of these ZI/salt blends over their semicrystalline polymer counterparts.

ZI/salt blends in motif I closely resemble superionic ceramics wherein zwitterionic crystallites may promote long-range transport of ionic species through a hopping mechanism. We have investigated the ionic conductivity of zwitterions with a smaller composition of salt added to the electrolyte such that the structure of the zwitterion remains dominated by crystallites. Despite the crystalline nature of the resulting electrolyte, there is significant ionic conductivity consistent with superionic transport. We find that a significant portion of the ionic conductivity can be attributed to lithium motion with a calculated lithium selectivity of 0.73. Similarly, the ZIs studied by Pringle and co-workers also displayed significant lithium conductivity despite their crystalline nature. They also observe mobility of both Li and TFSI; however, they see significantly reduced selectivity for lithium (t_+ = 0.29, though this still exceeds the selectivity of many electrolytes). Ohno also found a range of selectivity for similar crystal-forming zwitterions doped with lithium salts, ranging from ∼0.2 to 0.56. These wide variations in selectivity are not currently well understood; however, they are likely highly dependent on the association strength between the mobile ions and the

https://doi.org/10.1021/acspolymersau.2c00024
ACS Polym. Au 2022, 2, 430−448

zwitterionic matrix. These discrepant values of selectivity may also be partially explained by the experimental difficulties of accurately determining the selectivity; Balsara and co-workers have demonstrated these challenges.[1]

At higher salt loadings, only a T_g is seen, suggesting a glass-forming fluid (motif II) with distinct conduction and mechanical properties from the zwitterionic crystal (motif I). The behavior of ZI displaying structural motif II has been extensively characterized by Ohno who primarily studied nearly equimolar blends of ZI/salt in a wide variety of zwitterion and salt identities.[112,121,123] Ohno typically found that these blends displayed a T_g that is relatively insensitive to salt loading but may vary significantly based on salt and ZI identity. Pringle and co-workers[122] (Figure 6B) found that motif II is present across the salt concentration region of 20 to 70 mol % with coexistence of motif I+II at 10 mol % salt and coexistence of motifs II+III at 80−90 mol %. We (Figure 6C) also found similar behavior in blends of ZI/LiTFSI through X-ray scattering studies. Motif II is evident in our X-ray scattering data from the disappearance of ordered, Bragg-like reflections and their replacement with broad, liquidlike peaks. We show that multiple characteristic length scales exist in motif II (Figure 6C): two correlation length scales of $q_2 \sim 7$ Å and $q_3 \sim 4.5$ Å correspond to the packing of the disordered electrolyte. These two separate correlation peaks may arise from large differences in ion diameters, leading to slight ordering within the liquid phase, though more investigation is required to understand the liquidlike packing of these materials. At higher salt concentrations, we find that another larger correlation length scale arises at $q_1 \sim 20$ Å, which resembles the "ionomer peak" that emerges at high salt loadings of ions in organic polymer matrices. The emergence of this peak at high salt loadings suggests that similar amorphous salt-rich regions (ionic aggregates) form in the electrolyte; however, the salt concentration before aggregation is much higher than typical for ionomers (<3−10 mol % depending on the backbone identity),[15,124] likely because the dielectric contrast between zwitterion and salt is significantly reduced compared to zwitterion/organic polymer blends.

It is anticipated that when disordered, these ZI materials will display liquidlike mechanical and transport properties. This appears to be mostly true; however, some gaps in our understanding of conduction in this region remain. Ohno and co-workers have extensively investigated the ionic conductivity of these disordered electrolytes.[112,121,123] They find that conductivity roughly follows a WLF-like trend and appears to collapse based on glass transition temperatures across various zwitterions. These observations suggest that local ion dynamics play a critical role in promoting ionic conductivity. Future work investigating the Walden-plot behavior of these materials may be useful in determining the transport mechanism of these electrolytes. Further, despite being low molecular weight fluids above their glass transition temperatures, these materials display tremendous rigidity that approaches glassy behavior. The origin of this rigidity is not yet understood, but it may also have implications for their application as solid electrolytes.

At high salt concentrations, the zwitterion composition is small and the structure is dominated by the added salt, resulting in transport behavior that is likely dominated by regimes of motif II. This situation resembles polymer-in-salt electrolytes or high concentrations of salts in ILs where the majority of the electrolyte is comprised of crystalline salts with small disordered regions with very high carrier concentrations. Pringle observes the coexistence of motifs II+III at salt compositions ranging from 80 to 90 mol %. Although we do not observe this region for our blends of ZI/LiTFSI, we do see a wide region of this behavior for other salts such as NaCl and LiCl. Ion transport in the coexistence region of motifs II+III is likely to resemble transport of salt and ionic liquid blends at high salt concentrations, though no studies have sufficiently probed this region. Pringle observed that the conductivity in this high salt region can also be quite high, though the transport mechanism and selectivity are not currently known in this region. We believe that these solid electrolytes could be fruitful ion transport hosts and we suggest that this area requires additional study.

Ordering of zwitterions also occurs at a longer length scale in zwitterions that contain a significant nonpolar fraction such as alkyl tails. This ordering has been shown to have useful properties for promoting proton mobility; however, the relevance of these channels for other carrier ions is yet unknown. ZIs comprised of a highly polar headgroup and nonpolar tail can assemble into thermodynamically favored states that display order over the 1−3 nm length scale.[125−127] The structure resembles those seen in ionic liquids with hydrophobic tails, where a variety of liquid crystalline (smectic, nematic, etc.) and long-range ordered (micellar, cubic, hexagonal, and gyroidal) structures are observed at characteristic length scales of ∼10 nm. Ordered morphologies such as double-gyroid and aligned cylinder mesostructures may provide conduction pathways for ions, allowing ion motion even as fluidlike relaxation of the electrolyte is arrested.[125,127] These ion-carrying pathways may be capable of promoting superionic conduction. To our knowledge, there have not been any attempts to leverage a similar mechanism for the transport of larger ions than protons, but this could potentially provide an alternative mechanism for superionic transport in zwitterions by engineering larger length scale voids.

2.2. Polymers Based on Packing Frustration and Intrinsic Free Volume Promote Transport Through Voids

Packing frustration, especially the frustrated packing of rigid polymers, can also promote decoupled transport by imparting free volume through which ions can opportunistically hop. This has already been well appreciated in membrane gas transport applications; work from the Freeman group[128] and others[129] has shown that glassy polymers with very high fractional free volume exhibit exceptionally high permeabilities. In these materials, transport occurs through a static percolated network of free volume sites, enabling diffusion without the need for rearrangement of the membrane. Sokolov and co-workers have demonstrated that similar concepts apply in ion conducting polymers.[130] They have shown[7] that the fragility (a measure of packing frustration defined as $\text{fragility} = \left[\frac{\partial \log \tau_\alpha}{\partial (T_g/T)}\right]_{T=T_g}$) inversely correlates with the coupling exponent m (see section 1.4 for the definition of m). This relationship suggests that materials with greater extents of packing frustration may exhibit significant decoupling of ion transport from the liquid relaxation of the electrolyte. This may be rationalized by considering the free volume of fragile polymers, where more fragile, packing frustrated chains are unable to efficiently pack, leaving significant unstructured free volume in the material. Although frustrated, fragile chains are typically less able to create free volume for ion motion via a

https://doi.org/10.1021/acspolymersau.2c00024
ACS Polym. Au 2022, 2, 430−448

relaxation mechanism, and the static free volume in these systems can be sufficient to enable hopping-like transport of ions as illustrated in Figure 7B. While demonstrated ionic

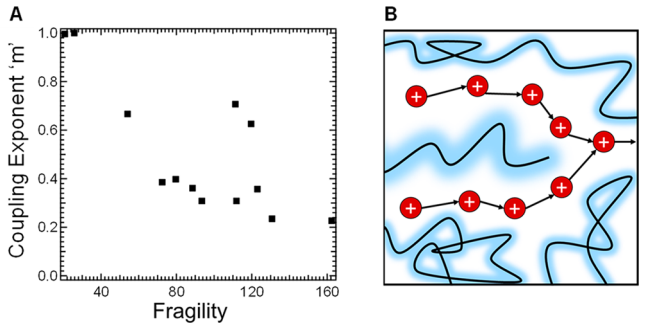

Figure 7. (A) Sokolov and co-workers studied a variety of SPE hosts and found a positive correlation between the decoupling exponent (m, where m is defined in Section 1.4 to be the slope of the Walden-plot curve) and polymer fragility. This suggests that more packing-frustrated materials display less coupling between conductivity and segmental motion. (B) The free volume channels of an electrolyte provide a network of vacancies through which ions can opportunistically hop. Data from Sokolov and co-workers.[130]

conductivities in these glassy systems are still modest, they have the potential for both high performance and less temperature-sensitivity than idealized liquid electrolytes.

While designing for ion diffusion through intrinsically porous polymers offers a promising means to impart superionic transport, one outstanding challenge arises from the limited solubility of dissociated ions in many packing-frustrated polymers. For instance it has been shown that while semirigid styrene-derived polymer electrolytes have very high decoupling ($m \sim 0.67$[27]), they do not demonstrate superionic conductivity under most conditions. This is due to poor salt solubility which reduces the concentration of charge carriers (low values of ξ). Many such rigid polymer electrolytes indeed show evidence of decoupling; however, this decoupling often only results in superionic transport when the ion concentration is renormalized by the extent of ion dissociation. Nonetheless, packing frustration presents an excellent opportunity to generate SPEs with high conductivity and rigidity, providing these solubility limitations can be overcome. Several authors report rigid SPEs that have attained conductivities suitable for applications based on this principle, demonstrating the potential promise of this approach.[131−134] This suggests a connection between materials that may superionically transport ions and materials developed for gas transport as both require free volume domains that percolate over large length scales. The well-developed literature in these areas could be used to further inspire materials design in these SPEs.[135,136] We suggest that future studies should investigate whether the free volume sites in materials such as poly(benzimidazoles)[137] or polyimides containing hard pentiptycene segments[138] can produce similar decoupling and whether salt solvation can be achieved in these materials.

2.3. Transport of Ions Through Nanostructured Channels

Although the ideal liquid mechanism of conductivity requires dynamical creation of free volume elements to generate a pathway for ion transport and ordering is typically associated with reduced mobility within electrolytes, proper arrangement of ion solvation sites and free volume can lead to high ionic conductivity. In particular, the constrained nature of diffusion in channels, the highly correlated nature of charge transport, and the prevention of ion backflow in channels may all lead to improved performance in materials with nanoscale structure.[44] Furthermore, transport in constrained channels can lead to selectivity rules that are sensitive to ion size. This provides an opportunity to improve selectivity for alkali metal ions since these ions are typically smaller than their counterions. Theoretical models suggest that ion channels can improve ion dynamics by concentrating ion motion along one-dimensional pathways given low free energy barriers and percolated paths for ion diffusion.[44] A variety of experimental approaches have been developed to generate ion transport pathways in electrolytes.

2.3.1. Co-crystalline Structures of Salts and Ions Can Provide Ion Transport Pathways. Although PEO conventionally displays its highest conductivity in the amorphous state; even this canonical electrolyte can display fast ion transport rates in a carefully engineered crystalline state. Reports by Bruce and co-workers[53,139] indicate that systems comprised of low-molecular weight PEO and salts ($LiXF_6$ where X = P, As, Sb, or $LiClO_4$) can cocrystallize to generate well-defined ionic channels whereby the ether oxygens of PEO wrap around lithium ions in tubelike formations with the anions excluded from these channels. These structures are confirmed with X-ray crystallography of the polymer-salt complexes, finding that well-defined Bragg reflections corresponding to the tubelike structure can be attained. Furthermore, they demonstrate appreciable ionic conductivity of these crystallites, despite the evident arrested segmental motion of the polymers. It is further shown that the ionic conductivity of this electrolyte even exceeds the conductivity of the equivalent amorphous-phase PEO, demonstrating the efficacy of this method to generate mechanically robust SPEs. A further advantage of these electrolytes is their excellent selectivity. Since the ion channels of the electrolyte effectively exclude anion motion, there is no free path for anion motion, resulting in excellent selectivity for lithium. Bruce and co-workers confirm this observation by NMR measurements, finding no evidence of anion mobility, corresponding to $t_+ = 1$.

Similar to this polymeric case, some reports indicate that crystalline complexes of salt and small organic molecules may also promote fast, selective transport of ions though crystallites.[140] For example, complexes of lithium bis(trifluoromethanesulfonimide) with dimethoxybenzene groups,[141] boron-containing molecules with glyme side chains,[142] and diamines[143] crystallize to form compounds with lithium and its counterion included in the crystal structure of the resulting electrolyte. These cocrystals display long-range transport pathways that conduct ions in the absence of structural rearrangement. These complexes have been shown to attain moderately high ionic conductivities $\sim 10^{-5}$ S/cm at 60 °C despite being totally crystalline. Recent work from Schaefer and co-workers has demonstrated a similar principle in single-ion conducting electrolytes consisting of sulfonamide ions with alkyl spacer tails. These electrolytes demonstrate crystalline order through scattering and calorimetric analysis. Despite this nature they display fast ion transport exceeding 1 mS/cm at elevated temperatures. Although the authors do not characterize the selectivity of the electrolyte, they suggest that it may approach unity based on the molecular structure of the electrolyte.[144]

https://doi.org/10.1021/acspolymersau.2c00024
ACS Polym. Au 2022, 2, 430−448

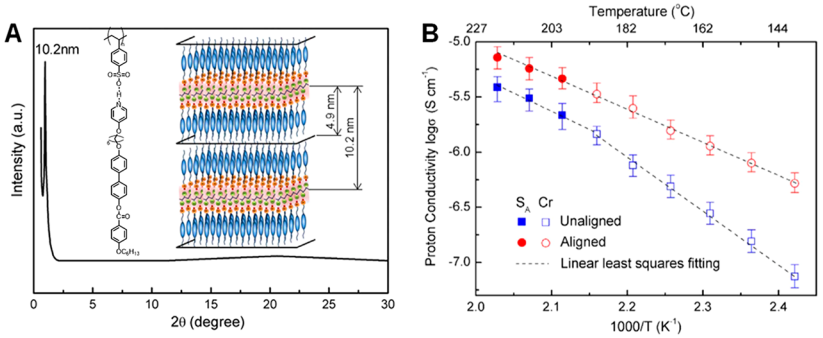

Figure 8. (A) Structural analysis of a liquid crystal/polymer adduct indicates chain packing where the anionic liquid crystalline moieties preferentially pack near the polymer backbones to form layered sheets. (B) The proton conductivity of this liquid crystal adduct shows alignment dependence, suggesting the importance of a nonhomogeneous transport mechanism. Reprinted with permission from ref 146. Copyright 2017 Elsevier.

2.3.2. Liquid Crystals and Liquid Crystalline Polymers Can Arrange to Create Ion Channels. Liquid crystalline (LC) moieties offer an excellent opportunity to simultaneously promote order and high conductivity, due to the structured nature of the mesogenic units and packing frustration from the rigid nature of these moieties. The simplest examples are nematic or smectic mesophases formed by rigid rodlike small molecules. However, bicontinuous cubic structures with high degrees of percolation for ion transport can be accessed through many design choices including lengths of alkyl linkers or tails, placement and strength of ionic or polar functionality, and selection of solvent or polymer environment.[125,145] For practical application in electrochemical devices, LCs exhibit the most useful nanostructures when they are imbedded in SPE systems. Here we focus on the ion conductive properties of polymers that are structured by small molecule LC additives and side chain liquid crystalline polymers.

Ionic interactions between LC additives and SPEs result in ionophilic channels capable of promoting ion conduction without relaxation of the polymer chain. In one manifestation, ionophilic head groups of LCs align near polymer backbones creating a 1D-layered structure that promotes conductivity when the layers are well-aligned.[146−148] For example, Yang et al.[149] observed the formation of ionic nanochannels through complexation of biphenyl benzoate-based pyridinium cationic stiff mesogens (Figure 8A inset) and the anionic functionalities of poly(styrenesulfonate) (Figure 8A). Evidence of a hopping mechanism through the nanochannels is obtained from both the relatively high conductivity of protons through the system at the polymer T_g (139 °C) and the increase in conductivity when channels were aligned (Figure 8B). Interestingly, these authors find that a change in the scaling of conductivity with temperature in the unaligned system occurs at ∼190C, which is coincident with the observed transition from nematic (Cr) to smectic (S_A), further emphasizing the importance of the alignment of these channels.

This approach has primarily been applied to proton conductors; however, application to metal ion conduction has also been demonstrated. For example, mixtures of PEO with the LC salt sodium tetracyanoquinodimethane has been reported to have a sodium ion conductivity above 3 mS/cm at room temperature, much higher than PEO under the same conditions,[150] even when prepared in the amorphous state. Similar to the protic cases, the conductivity of the film shows alignment-dependent conductivity, suggesting that the percolation of nanochannels plays a crucial role in ion transport performance. In another approach, polymeric LCs drive the nanostructural formation of ionic liquid crystalline grains leveraged between rigid-rod polyamide chains.[151] This lyotropic LC assembly of the polyamide effectively templates the formation of a percolated nanocrystalline network. Lithium ions were shown to migrate via a hopping mechanism through defect structures in the alloy.

Another approach is to utilize polymer-bound liquid-crystalline moieties to organize ionophilic domains capable of transporting ions. Wright and co-workers have studied polymers comprised of polyether backbone chains with regularly spaced alkyl side chains pendant to the backbone.[150,152,153] The alkyl side chains of these materials can cocrystallize inter- and intramolecularly with other side chains within the electrolyte, resulting in nonconductive alkyl crystallites with ethylene oxide chains located at the crystal periphery. Although these electrolytes are very rigid due to their high crystallinities, they exhibit high ionic conductivities up to 10^{-2} S/cm. Ion transport is hypothesized to occur through the two-dimensional interface layers, rather than through the crystallites. The highly anisotropic conductivity (10^{-4} S/cm along ion channels and $<10^{-12}$ perpendicular to the channels) of the aligned electrolyte confirms this conductivity mechanism. A similar mechanism and approach was employed by McHattie et al.,[154−156] who studied polyethers with regularly spaced mesogenic groups which align in a similar fashion to the alkyl chains employed by Wright and co-workers.[150,152,153] These materials also display highly anisotropic conduction that occurs at fast rates in spite of the frozen structure of the electrolyte, displaying no significant change in conductivity, below the T_g of the polymer. These authors hypothesize that the ion transport in these electrolytes is also highly selective; however, we are not aware of any measurements of selectivity for these systems.

2.3.3. Ion Transport Pathways Created by Ionic Aggregation. While ionic aggregation of the mobile cations is deleterious to conduction in conventional liquids, ionic aggregation of the charged components of the SPE can lead to nanostructured channels that conduct ions without relaxation of the bulk material. The mechanism of ion transport depends strongly on the morphology and percolated nature of the aggregates which are in turn impacted by factors such as polymer architecture, ion diameters, and polymer and ion chemistries. Molecular dynamics simulations suggest that extended stringlike aggregates that percolate through the material[157−161] may eliminate the need for ions to hop

https://doi.org/10.1021/acspolymersau.2c00024
ACS Polym. Au 2022, 2, 430−448

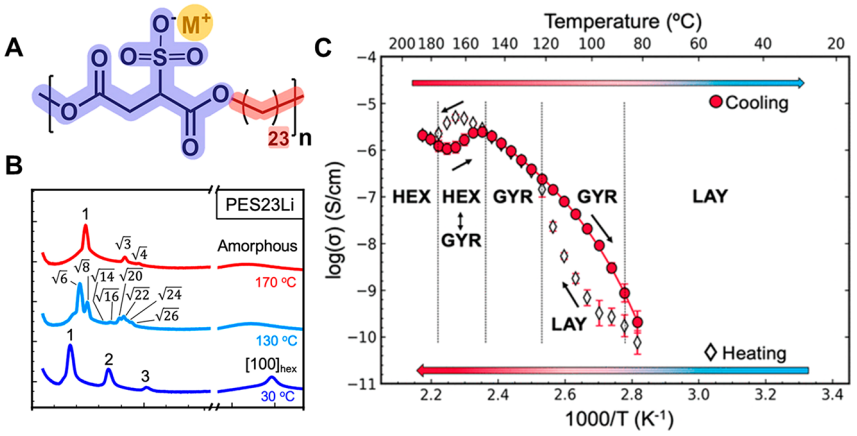

Figure 9. (A) Winey and co-workers used condensation polymerization to prepare materials with precise spacing between ionic groups. (B) Small-angle X-ray scattering experiments reveal the presence of layered, gyroidal, and hexagonally close-packed morphologies. The wide-angle experiments show crystallinity of the polyethylene chains at low temperature. (C) The ionic conductivity was measured on a heating-cooling cycle of this electrolyte. The ionic conductivity increases significantly during the transition between layered structures and gyroidal structures. At higher temperatures, the transition between gyroid and hexagonally close packed cylinders results in a reduction in the ionic conducitivity. The same trend is seen upon cooling. Adapted from ref 164. Copyright 2020 American Chemical Society.

between ion clusters and instead promote high conductivity if the clusters present a locally dynamic environment for ion movement. Partial decoupling of ion transport from the segmental dynamics of the nonpolar domains of the SPE is possible under these conditions. Though transport within clusters may be subject to similar transport constraints such as correlated ion motions and low selectivity for cations of interest, simulations suggest that ion transport in confinement may be improved compared to bulk liquid motion. This may offer a means to tune transport in confined environments. While significant effort has been expended to characterize the structure and interconnectedness within aggregates, fast and effective transport requires both percolation and rapid local dynamics within aggregates, which is also challenging to attain.

This mechanism of intra-aggregate transport has led to concerted efforts to generate percolated aggregate shapes and higher ionic conductivities. One strategy to generate percolated structures has focused on the nature of the ion attachment. It has been shown that "ionenes" (polymers with the ion included in the backbone rather than being tethered to it) display faster T_g-normalized ion transport than their ionomer counterparts.[162,163] Studies have also demonstrated that these ionenes result in more percolated ionic structures.[158] Ion aggregation is also intimately tied to the dielectric constant of the electrolyte; however, joint experimental-simulation studies have shown that the dielectric constant, while impacting the extent of ion aggregation, has a limited impact on the rate of ion transport as long as the aggregates are percolated through the electrolyte.[15]

Tuning the structure of aggregates to generate highly percolated structures greatly enhance the degree of decoupled transport in these electrolytes. SPEs consisting of ionic groups separated a precise distance by a nonpolar alkyl chain (Figure 9A)[164−167] have been studied by Winey and co-workers. The combination of high polarity contrast and the regular ion spacing of these materials results in ordered packings of ionic domains that can conduct dissociated ions. Winey and co-workers have similarly demonstrated a variety of morphologies, including layered, hexagonal, and gyroid structures (Figure 9B). They found that these materials exhibit morphology-dependent ionic conductivity trends (Figure 9C), consistent with the described mechanism whereby ionic conductivity depends on the connectivity of the ion-transporting channels. Similarly, Abbott and co-workers demonstrated with molecular dynamics simulations that well-defined side-chain polymers could self-assemble into precise ionic layer structures.[124] Their results were experimentally validated in collaboration with McCloskey and co-workers who generated poly(allyl glycidyl ether)-based materials with well-defined ionic layer structures.[168] Although these aggregates are structurally percolated, they do not display intra-aggregate ion transport due to the rigid nature of the ionic aggregates in the system.

The ion aggregates formed in such systems can be locally fluid, amorphous solids, or crystalline. In most systems demonstrating high ionic conductivity, the aggregates are fluidlike. However, conceptually it is possible for a SPE to support high conductivity if the ion aggregates are amorphous solids or crystals with sufficient free volume, vacancies, or interstitial sites to enable rapid ion motion. The nature of the aggregates can also be influenced by the addition of plasticizing molecules or polymers that retain the shape of the aggregate while enabling faster fluidlike transport. For instance Paren et al.[169] recently reported on styrene-based lithium single-ion conductors that strongly aggregate. Although the aggregates in this system are expected to structurally percolate, the transport through the ion channels in the absence of plasticizer is slow due to strong ion-polymer interactions and collapsed ion channels; however, the addition of plasticizing, low molecular weight PEO broadens the ion channels and allows for greater ion dissociation. In this case, the plasticizer acts to change the transport rate through the ion channels while disrupting their structure. Similarly, the transport through ion channels in layered electrolytes consisting of a PEO backbone with alkyl side-chains could be improved by greater than 2 orders of magnitude when blended with polar polymers[170,171] or plasticizers,[172] which effectively swelled the ionic channels and increased their fluidity. This suggests that effective design of ion channels must effectively consider the connectivity of channels as well as the mobility in these channels, which relates to their size as well as the energy barrier for activated transport within these channels.

https://doi.org/10.1021/acspolymersau.2c00024
ACS Polym. Au 2022, 2, 430−448

3. OUTSTANDING QUESTIONS

3.1. Large and Multivalent Ions

The motion of large and multivalent ions is of increasing technological interest as new battery chemistries such as those based on Mg^{2+},[173] Zn^{2+},[174] and Al^{3+}[175] emerge as possible sustainable, low-cost, more abundant, and safe alternatives to lithium-ion battery cells. One challenge for such battery chemistries is the low mobility of multivalent ions in traditional electrolytes;[176] even liquid electrolytes generally have low mobilities for such cations. Although multivalent ions are generally less reactive and may be inherently safer, the need for ion conductors that are selective for cation motion is pressing in these materials due to the large interfacial polarization effects that plague multivalent cation cells in the literature. As in lithium, it may be advantageous to decouple the transport of multivalent ions from the mobility of the matrix. However, nearly all the focus so far on this activity has been on lithium or sodium ions. Two clear challenges facing transport of multivalent ions are their large size and strong interactions with the matrix.

The size of multivalent ions is especially relevant because many mechanisms to decouple ion transport from segmental mobility rely on creating void spaces large enough for ionic hopping. The size of such voids would need to be considerably larger to promote superionic motion of multivalent ions. Nonetheless, this challenge is not insurmountable as superionic transport of Mg^{2+}[177−179] has already been reported in ceramic materials. Frustrated chain packing may be useful in conducting large ions since this approach generates a range of void sizes that can be exploited, instead of the structured and discrete voids generated by other approaches. Another possible approach to creating channels for superionic conduction of large ions could be in generating cocrystalline structures of ions and matrix molecules. It is known that larger cations can coordinate with cyclic crown ethers,[180] which may present an opportunity to generate nanochannels inspired by the work of Bruce and co-workers.[139]

Even in the presence of an appropriate transport pathway, the motion of multivalent ions through an electrolyte can be limited if matrix-ion interactions are strong. Size-selectivity approaches (such as those mentioned in Section 2) are less effective with larger multivalent ions. Indeed, in amorphous PEO, the strong coordination between the ether oxygens and magnesium results in low selectivity ($t_+ < 0.1$) for magnesium ions.[181,182] Consequently, tuning ion-matrix interactions may be even more crucial in the design of multivalent ion conductors, focusing on labile interactions to promote facile hopping between solvation sites. It could also be useful to include labile solvating compounds in such electrolytes such as the replacement of ethers with thioethers, or using bulky ionic-liquid inspired ions to improve mobility within ionic aggregates.

3.2. Practical Aspects of Ion Transport in Structured Electrolytes

Although most studies in the literature simply measure the ionic conductivity and the selectivity of an electrolyte, a real electrolyte must support high cell current by promoting high fluxes of redox active ions and allowing for interfacial reactions with the electrode to occur. As such, high ionic conductivity is insufficient to ensure satisfactory performance of a battery or electrochemical device. Here we focus on the failure of an electrolyte to withstand the electrochemical environment and limitations at the electrode−electrolyte interface.

For the ionic conductivity to be representative of the flux of a resistor, the resistor must be Ohmic in the range of interest.[1] Ohm's law will typically fail when an electrolyte experiences a chemical degradation as a function of the applied voltage that impacts the transport properties of the electrolyte. As such, potential electrolytes should be studied for their voltage stability in tandem with their ionic conductivity.[183,184] Stability in the presence of lithium metal should be demonstrated early on in the development of these new classes of material, since failing to focus on stability at an early stage in development of battery materials has consistently failed to deliver truly robust and long-lasting components. Both bulk and interfacial investigations of electrolyte stability in the presence of lithium and under thermal and voltage stresses should be evaluated early on in evaluation of materials.

Although ion transport is essential to the performance of electrochemical cells, the redox-active species must also undergo electrochemical reactions for the cell to function. In liquid electrolytes, the solvated material is electrochemically available for reactions that lead to current within the cell. However, issues at the interface are common, especially in rigid superionic ceramics that may experience poor interfacial contact or hindered electroactivity at the interface due to the strong binding of lithium to the interface.[185] This issue can also arise in block copolymer electrolytes where the redox active species is concentrated within the conducting block domains of the electrolyte, leading to reduced utilization of the electrode interface for reactions.[186] Many of the SPE systems described in this perspective have never been investigated in a complete working cell. As such, fundamental transport measurements, bulk and interfacial stability investigations, and extended testing in full electrochemical cells will all be required to implement emerging SPEs into real devices.

3.3. Conclusions

This perspective provides a critical examination of the ideal liquid transport mechanism in SPEs, which is a widely held view of how ions move in such systems, finding that application of this principle broadly across polymers insufficiently describes the diverse transport mechanisms at play. The decoupling between ion transport and polymer segmental mobility is practically useful, reducing the temperature dependence of ionic conductivity, which is critical to electrochemical device operation over a broad temperature range, and allowing independent tuning of mechanical and ion transport properties. Several strategies were reviewed to promote the ion-matrix decoupling. Generally, we find three features are required for decoupling: (1) an inhomogeneity that allows for ion motion distinct from segmental motion, such inhomogeneities can be disordered and arise from packing frustration or highly ordered, resulting from crystallization or self-assembly; (2) labile ion-matrix interactions to promote activated transport between sites; and (3) facile small-length scale motion within channels created by the inhomogeneity, e.g., the paddlewheel effect observed in superionic ceramic materials.

AUTHOR INFORMATION

Corresponding Author

Rachel A. Segalman − *Department of Chemical Engineering, Materials Research Laboratory, and Mitsubishi Chemical*

https://doi.org/10.1021/acspolymersau.2c00024
ACS Polym. Au 2022, 2, 430−448

Center for Advanced Materials, University of California, Santa Barbara, California 93106, United States; Materials Department, University of California Santa Barbara, Santa Barbara, California 93106, United States; orcid.org/0000-0002-4292-5103; Email: Segalman@ucsb.edu

Authors

Seamus D. Jones − *Department of Chemical Engineering, Materials Research Laboratory, and Mitsubishi Chemical Center for Advanced Materials, University of California, Santa Barbara, California 93106, United States*

James Bamford − *Materials Research Laboratory and Mitsubishi Chemical Center for Advanced Materials, University of California, Santa Barbara, California 93106, United States; Materials Department, University of California Santa Barbara, Santa Barbara, California 93106, United States*

Glenn H. Fredrickson − *Department of Chemical Engineering, Materials Research Laboratory, and Mitsubishi Chemical Center for Advanced Materials, University of California, Santa Barbara, California 93106, United States; Materials Department, University of California Santa Barbara, Santa Barbara, California 93106, United States;* orcid.org/0000-0002-6716-9017

Complete contact information is available at: https://pubs.acs.org/10.1021/acspolymersau.2c00024

Notes

The authors declare the following competing financial interest(s): G.H.F is a paid board member and advisor of Misubishi Chemical Holdings Corporation.

■ ACKNOWLEDGMENTS

The research reported here was primarily supported by the National Science Foundation (NSF) through the Materials Research Science and Engineering Center at UC Santa Barbara, DMR-1720256 (IRG-2). S.D.J. also acknowledges financial support from the Mitsubishi Chemical Center for Advanced Materials (MC-CAM). S.D.J. wishes to acknowledge Jack Douglas for helping to clarify concepts regarding the decoupling exponent.

■ REFERENCES

(1) Galluzzo, M. D.; Maslyn, J. A.; Shah, D. B.; Balsara, N. P. Ohm's law for ion conduction in lithium and beyond-lithium battery electrolytes. *J. Chem. Phys.* **2019**, *151* (2), 020901.

(2) Bocharova, V.; Sokolov, A. P. Perspectives for Polymer Electrolytes: A View from Fundamentals of Ionic Conductivity. *Macromolecules* **2020**, *53* (11), 4141−4157.

(3) Hallinan, D. T.; Balsara, N. P. Polymer Electrolytes. *Annu. Rev. Mater. Res.* **2013**, *43* (1), 503−525.

(4) Bruce, P. G.; Vincent, C. A. Polymer electrolytes. *Journal of the Chemical Society, Faraday Transactions* **1993**, *89* (17), 3187−3203.

(5) Evans, J.; Vincent, C. A.; Bruce, P. G. Electrochemical measurement of transference numbers in polymer electrolytes. *Polymer* **1987**, *28* (13), 2324−2328.

(6) Marcus, Y.; Hefter, G. Ion Pairing. *Chem. Rev.* **2006**, *106* (11), 4585−4621.

(7) Nordness, O.; Brennecke, J. F. Ion Dissociation in Ionic Liquids and Ionic Liquid Solutions. *Chem. Rev.* **2020**, *120* (23), 12873−12902.

(8) Kirchner, B.; Malberg, F.; Firaha, D. S.; Hollóczki, O. Ion pairing in ionic liquids. *J. Phys.: Condens. Matter* **2015**, *27* (46), 463002.

(9) Hollóczki, O.; Malberg, F.; Welton, T.; Kirchner, B. On the origin of ionicity in ionic liquids. Ion pairing versus charge transfer. *Phys. Chem. Chem. Phys.* **2014**, *16* (32), 16880−16890.

(10) Harris, K. R. Can the Transport Properties of Molten Salts and Ionic Liquids Be Used To Determine Ion Association? *J. Phys. Chem. B* **2016**, *120* (47), 12135−12147.

(11) Ueno, K.; Tokuda, H.; Watanabe, M. Ionicity in ionic liquids: correlation with ionic structure and physicochemical properties. *Phys. Chem. Chem. Phys.* **2010**, *12* (8), 1649−1658.

(12) Stassen, H. K.; Ludwig, R.; Wulf, A.; Dupont, J. Imidazolium Salt Ion Pairs in Solution. *Chemistry − A European Journal* **2015**, *21* (23), 8324−8335.

(13) MacFarlane, D. R.; Forsyth, M.; Izgorodina, E. I.; Abbott, A. P.; Annat, G.; Fraser, K. On the concept of ionicity in ionic liquids. *Phys. Chem. Chem. Phys.* **2009**, *11* (25), 4962−4967.

(14) Schreiner, C.; Zugmann, S.; Hartl, R.; Gores, H. J. Fractional Walden Rule for Ionic Liquids: Examples from Recent Measurements and a Critique of the So-Called Ideal KCl Line for the Walden Plot. *Journal of Chemical & Engineering Data* **2010**, *55* (5), 1784−1788.

(15) Schauser, N. S.; Grzetic, D. J.; Tabassum, T.; Kliegle, G. A.; Le, M. L.; Susca, E. M.; Antoine, S.; Keller, T. J.; Delaney, K. T.; Han, S.; Seshadri, R.; Fredrickson, G. H.; Segalman, R. A. The Role of Backbone Polarity on Aggregation and Conduction of Ions in Polymer Electrolytes. *J. Am. Chem. Soc.* **2020**, *142* (15), 7055−7065.

(16) Jones, S. D.; Schauser, N. S.; Fredrickson, G. H.; Segalman, R. A. The Role of Polymer−Ion Interaction Strength on the Viscoelasticity and Conductivity of Solvent-Free Polymer Electrolytes. *Macromolecules* **2020**, *53* (23), 10574−10581.

(17) Grindy, S. C.; Learsch, R.; Mozhdehi, D.; Cheng, J.; Barrett, D. G.; Guan, Z.; Messersmith, P. B.; Holten-Andersen, N. Control of hierarchical polymer mechanics with bioinspired metal-coordination dynamics. *Nat. Mater.* **2015**, *14* (12), 1210−1216.

(18) Shen, K.-H.; Hall, L. M. Effects of Ion Size and Dielectric Constant on Ion Transport and Transference Number in Polymer Electrolytes. *Macromolecules* **2020**, *53* (22), 10086−10096.

(19) Savoie, B. M.; Webb, M. A.; Miller, T. F. Enhancing Cation Diffusion and Suppressing Anion Diffusion via Lewis-Acidic Polymer Electrolytes. *J. Phys. Chem. Lett.* **2017**, *8* (3), 641−646.

(20) Fan, F.; Wang, Y.; Hong, T.; Heres, M. F.; Saito, T.; Sokolov, A. P. Ion Conduction in Polymerized Ionic Liquids with Different Pendant Groups. *Macromolecules* **2015**, *48* (13), 4461−4470.

(21) Zhao, Y.; Bai, Y.; Li, W.; An, M.; Bai, Y.; Chen, G. Design Strategies for Polymer Electrolytes with Ether and Carbonate Groups for Solid-State Lithium Metal Batteries. *Chem. Mater.* **2020**, *32* (16), 6811−6830.

(22) Pitzer, K. S. Electrolytes. From dilute solutions to fused salts. *J. Am. Chem. Soc.* **1980**, *102* (9), 2902−2906.

(23) Mao, G.; Saboungi, M.-L.; Price, D. L.; Armand, M.; Mezei, F.; Pouget, S. α-Relaxation in PEO−LiTFSI Polymer Electrolytes. *Macromolecules* **2002**, *35* (2), 415−419.

(24) Ma, Y.; Doyle, M.; Fuller, T. F.; Doeff, M. M.; De Jonghe, L. C.; Newman, J. The Measurement of a Complete Set of Transport Properties for a Concentrated Solid Polymer Electrolyte Solution. *J. Electrochem. Soc.* **1995**, *142* (6), 1859−1868.

(25) Gouverneur, M.; Schmidt, F.; Schönhoff, M. Negative effective Li transference numbers in Li salt/ionic liquid mixtures: does Li drift in the "Wrong" direction? *Phys. Chem. Chem. Phys.* **2018**, *20* (11), 7470−7478.

(26) Pesko, D. M.; Timachova, K.; Bhattacharya, R.; Smith, M. C.; Villaluenga, I.; Newman, J.; Balsara, N. P. Negative Transference Numbers in Poly(ethylene oxide)-Based Electrolytes. *J. Electrochem. Soc.* **2017**, *164* (11), E3569−E3575.

(27) Wang, Y.; Fan, F.; Agapov, A. L.; Yu, X.; Hong, K.; Mays, J.; Sokolov, A. P. Design of superionic polymers—New insights from Walden plot analysis. *Solid State Ionics* **2014**, *262*, 782−784.

(28) Voronel, A.; Veliyulin, E.; Machavariani, V. S.; Kisliuk, A.; Quitmann, D. Fractional Stokes-Einstein Law for Ionic Transport in Liquids. *Phys. Rev. Lett.* **1998**, *80* (12), 2630−2633.

(29) Becher, M.; Becker, S.; Hecht, L.; Vogel, M. From Local to Diffusive Dynamics in Polymer Electrolytes: NMR Studies on Coupling of Polymer and Ion Dynamics across Length and Time Scales. *Macromolecules* **2019**, *52* (23), 9128−9139.
(30) Maitra, A.; Heuer, A. Cation Transport in Polymer Electrolytes: A Microscopic Approach. *Phys. Rev. Lett.* **2007**, *98* (22), 227802.
(31) Borodin, O.; Smith, G. D. Mechanism of Ion Transport in Amorphous Poly(ethylene oxide)/LiTFSI from Molecular Dynamics Simulations. *Macromolecules* **2006**, *39* (4), 1620−1629.
(32) Dam, T.; Jena, S. S.; Pradhan, D. K. The ionic transport mechanism and coupling between the ion conduction and segmental relaxation processes of PEO20-LiCF3SO3 based ion conducting polymer clay composites. *Phys. Chem. Chem. Phys.* **2016**, *18* (29), 19955−19965.
(33) Druger, S. D.; Nitzan, A.; Ratner, M. A. Dynamic bond percolation theory: A microscopic model for diffusion in dynamically disordered systems. I. Definition and one-dimensional case. *J. Chem. Phys.* **1983**, *79* (6), 3133−3142.
(34) Nitzan, A.; Ratner, M. A. Conduction in Polymers: Dynamic Disorder Transport. *J. Phys. Chem.* **1994**, *98* (7), 1765−1775.
(35) Lonergan, M. C.; Nitzan, A.; Ratner, M. A.; Shriver, D. F. Dynamically disordered hopping, glass transition, and polymer electrolytes. *J. Chem. Phys.* **1995**, *103* (8), 3253−3261.
(36) Webb, M. A.; Savoie, B. M.; Wang, Z.-G.; Miller, T. F., III Chemically Specific Dynamic Bond Percolation Model for Ion Transport in Polymer Electrolytes. *Macromolecules* **2015**, *48* (19), 7346−7358.
(37) Diddens, D.; Heuer, A.; Borodin, O. Understanding the Lithium Transport within a Rouse-Based Model for a PEO/LiTFSI Polymer Electrolyte. *Macromolecules* **2010**, *43* (4), 2028−2036.
(38) Pedretti, B. J.; Czarnecki, N. J.; Zhu, C.; Imbrogno, J.; Rivers, F.; Freeman, B. D.; Ganesan, V.; Lynd, N. A. Structure−Property Relationships for Polyether-Based Electrolytes in the High-Dielectric-Constant Regime. *Macromolecules* **2022**, *55* (15), 6730−6738.
(39) Siqueira, L. J. A.; Ribeiro, M. C. C. Molecular dynamics simulation of the polymer electrolyte poly(ethylene oxide)/LiClO4. II. Dynamical properties. *J. Chem. Phys.* **2006**, *125* (21), 214903.
(40) Duan, Y.; Halley, J. W.; Curtiss, L.; Redfern, P. Mechanisms of lithium transport in amorphous polyethylene oxide. *J. Chem. Phys.* **2005**, *122* (5), 054702.
(41) Muller-Plathe, F.; van Gunsteren, W. F. Computer simulation of a polymer electrolyte: Lithium iodide in amorphous poly(ethylene oxide). *J. Chem. Phys.* **1995**, *103* (11), 4745−4756.
(42) Borodin, O.; Smith, G. D.; Geiculescu, O.; Creager, S. E.; Hallac, B.; DesMarteau, D. Li+ Transport in Lithium Sulfonylimide−Oligo(ethylene oxide) Ionic Liquids and Oligo(ethylene oxide) Doped with LiTFSI. *J. Phys. Chem. B* **2006**, *110* (47), 24266−24274.
(43) Deng, C.; Webb, M. A.; Bennington, P.; Sharon, D.; Nealey, P. F.; Patel, S. N.; de Pablo, J. J. Role of Molecular Architecture on Ion Transport in Ethylene oxide-Based Polymer Electrolytes. *Macromolecules* **2021**, *54* (5), 2266−2276.
(44) Muthukumar, M. Theory of Ionic Conductivity with Morphological Control in Polymers. *ACS Macro Lett.* **2021**, *10* (7), 958−964.
(45) Kang, P.; Wu, L.; Chen, D.; Su, Y.; Zhu, Y.; Lan, J.; Yang, X.; Sui, G. Dynamical Ion Association and Transport Properties in PEO−LiTFSI Electrolytes: Effect of Salt Concentration. *J. Phys. Chem. B* **2022**, *126* (24), 4531−4542.
(46) Fullerton-Shirey, S. K.; Maranas, J. K. Effect of LiClO4 on the Structure and Mobility of PEO-Based Solid Polymer Electrolytes. *Macromolecules* **2009**, *42* (6), 2142−2156.
(47) Mongcopa, K. I. S.; Tyagi, M.; Mailoa, J. P.; Samsonidze, G.; Kozinsky, B.; Mullin, S. A.; Gribble, D. A.; Watanabe, H.; Balsara, N. P. Relationship between Segmental Dynamics Measured by Quasi-Elastic Neutron Scattering and Conductivity in Polymer Electrolytes. *ACS Macro Lett.* **2018**, *7* (4), 504−508.
(48) Yoshida, K.; Manabe, H.; Takahashi, Y.; Furukawa, T. Correlation between ionic and molecular dynamics in the liquid state of polyethylene oxide/lithium perchlorate complexes. *Electrochim. Acta* **2011**, *57*, 139−146.
(49) Schauser, N. S.; Kliegle, G. A.; Cooke, P.; Segalman, R. A.; Seshadri, R. Database Creation, Visualization, and Statistical Learning for Polymer Li+-Electrolyte Design. *Chem. Mater.* **2021**, *33* (13), 4863−4876.
(50) Mindemark, J.; Lacey, M. J.; Bowden, T.; Brandell, D. Beyond PEO—Alternative host materials for Li+-conducting solid polymer electrolytes. *Prog. Polym. Sci.* **2018**, *81*, 114−143.
(51) Berthier, C.; Gorecki, W.; Minier, M.; Armand, M. B.; Chabagno, J. M.; Rigaud, P. Microscopic investigation of ionic conductivity in alkali metal salts-poly(ethylene oxide) adducts. *Solid State Ionics* **1983**, *11* (1), 91−95.
(52) Armand, M. Polymer solid electrolytes - an overview. *Solid State Ionics* **1983**, *9−10*, 745−754.
(53) Gadjourova, Z.; Andreev, Y. G.; Tunstall, D. P.; Bruce, P. G. Ionic conductivity in crystalline polymer electrolytes. *Nature* **2001**, *412* (6846), 520−523.
(54) Bruce, P. G.; Vincent, C. Polymer electrolytes. *Journal of the Chemical Society, Faraday Transactions* **1993**, *89* (17), 3187−3203.
(55) Borodin, O.; Smith, G. D. Mechanism of ion transport in amorphous poly (ethylene oxide)/LiTFSI from molecular dynamics simulations. *Macromolecules* **2006**, *39* (4), 1620−1629.
(56) Geng, Z.; Schauser, N. S.; Lee, J.; Schmeller, R. P.; Barbon, S. M.; Segalman, R. A.; Lynd, N. A.; Hawker, C. J. Role of Side-Chain Architecture in Poly(ethylene oxide)-Based Copolymers. *Macromolecules* **2020**, *53* (12), 4960−4967.
(57) Bennington, P.; Deng, C.; Sharon, D.; Webb, M. A.; de Pablo, J. J.; Nealey, P. F.; Patel, S. N. Role of solvation site segmental dynamics on ion transport in ethylene-oxide based side-chain polymer electrolytes. *Journal of Materials Chemistry A* **2021**, *9* (15), 9937−9951.
(58) Lee, B. F.; Kade, M. J.; Chute, J. A.; Gupta, N.; Campos, L. M.; Fredrickson, G. H.; Kramer, E. J.; Lynd, N. A.; Hawker, C. J. Poly(allyl glycidyl ether)-A versatile and functional polyether platform. *J. Polym. Sci. A Polym. Chem.* **2011**, *49* (20), 4498−4504.
(59) Strawhecker, K. E.; Manias, E. Crystallization Behavior of Poly(ethylene oxide) in the Presence of Na+ Montmorillonite Fillers. *Chem. Mater.* **2003**, *15* (4), 844−849.
(60) Ni'mah, Y. L.; Cheng, M.-Y.; Cheng, J. H.; Rick, J.; Hwang, B.-J. Solid-state polymer nanocomposite electrolyte of TiO2/PEO/NaClO4 for sodium ion batteries. *J. Power Sources* **2015**, *278*, 375−381.
(61) Feng, J.; Wang, L.; Chen, Y.; Wang, P.; Zhang, H.; He, X. PEO based polymer-ceramic hybrid solid electrolytes: a review. *Nano Convergence* **2021**, *8* (1), 2.
(62) Lehmann, M. L.; Yang, G.; Nanda, J.; Saito, T. Well-designed Crosslinked Polymer Electrolyte Enables High Ionic Conductivity and Enhanced Salt Solvation. *J. Electrochem. Soc.* **2020**, *167* (7), 070539.
(63) Li, W.; Pang, Y.; Liu, J.; Liu, G.; Wang, Y.; Xia, Y. A PEO-based gel polymer electrolyte for lithium ion batteries. *RSC Adv.* **2017**, *7* (38), 23494−23501.
(64) Gregorio, V.; García, N.; Tiemblo, P. Ionic Conductivity Enhancement in UHMW PEO Gel Electrolytes Based on Room-Temperature Ionic Liquids and Deep Eutectic Solvents. *ACS Applied Polymer Materials* **2022**, *4* (4), 2860−2870.
(65) Snyder, R. L.; Choo, Y.; Gao, K. W.; Halat, D. M.; Abel, B. A.; Sundararaman, S.; Prendergast, D.; Reimer, J. A.; Balsara, N. P.; Coates, G. W. Improved Li+ Transport in Polyacetal Electrolytes: Conductivity and Current Fraction in a Series of Polymers. *ACS Energy Letters* **2021**, *6* (5), 1886−1891.
(66) Goulart, G.; Sanchez, J.-Y.; Armand, M. Synthesis and electrochemical characterization of new polymer electrolytes based on dioxolane homo and co-polymers. *Electrochimica acta* **1992**, *37* (9), 1589−1592.
(67) Kumar, Y.; Hashmi, S. A.; Pandey, G. P. Lithium ion transport and ion−polymer interaction in PEO based polymer electrolyte plasticized with ionic liquid. *Solid State Ionics* **2011**, *201* (1), 73−80.

https://doi.org/10.1021/acspolymersau.2c00024
ACS Polym. Au 2022, 2, 430−448

(68) Suthanthiraraj, S. A.; Vadivel, M. K. Effect of propylene carbonate as a plasticizer on (PEO)50AgCF3SO3:SnO2 nanocomposite polymer electrolyte. *Applied Nanoscience* **2012**, *2* (3), 239−246.
(69) Shin, J.-H.; Henderson, W. A.; Passerini, S. PEO-Based Polymer Electrolytes with Ionic Liquids and Their Use in Lithium Metal-Polymer Electrolyte Batteries. *J. Electrochem. Soc.* **2005**, *152* (5), A978.
(70) Sharma, J. P.; Singh, V. Influence of high and low dielectric constant plasticizers on the ion transport properties of PEO: NH4HF2 polymer electrolytes. *High Perform. Polym.* **2020**, *32* (2), 142−150.
(71) Polu, A. R.; Singh, P. K. Improved ion dissociation and amorphous region of PEO based solid polymer electrolyte by incorporating tetracyanoethylene. *Materials Today: Proceedings* **2022**, *49*, 3093−3097.
(72) Li, Y.; Zhang, L.; Sun, Z.; Gao, G.; Lu, S.; Zhu, M.; Zhang, Y.; Jia, Z.; Xiao, C.; Bu, H.; Xi, K.; Ding, S. Hexagonal boron nitride induces anion trapping in a polyethylene oxide based solid polymer electrolyte for lithium dendrite inhibition. *Journal of Materials Chemistry A* **2020**, *8* (19), 9579−9589.
(73) Vishwakarma, V.; Jain, A. Enhancement of thermal transport in Gel Polymer Electrolytes with embedded BN/Al2O3 nano- and micro-particles. *J. Power Sources* **2017**, *362*, 219−227.
(74) Cai, Y.; Zeng, L.; Zhang, Y.; Xu, X. Multiporous sp2-hybridized boron nitride (d-BN): stability, mechanical properties, lattice thermal conductivity and promising application in energy storage. *Phys. Chem. Chem. Phys.* **2018**, *20* (31), 20726−20731.
(75) Tian, H.; Seh, Z. W.; Yan, K.; Fu, Z.; Tang, P.; Lu, Y.; Zhang, R.; Legut, D.; Cui, Y.; Zhang, Q. Theoretical Investigation of 2D Layered Materials as Protective Films for Lithium and Sodium Metal Anodes. *Adv. Energy Mater.* **2017**, *7* (13), 1602528.
(76) Wang, J.; Zhang, C.; Zhang, Y.; Xue, Z. Advances in host selection and interface regulation of polymer electrolytes. *J. Polym. Sci.* **2022**, *60* (5), 743−765.
(77) Heitjans, P.; Indris, S. Diffusion and ionic conduction in nanocrystalline ceramics. *J. Phys.: Condens. Matter* **2003**, *15* (30), R1257.
(78) Sun, J.; Clark, B. K.; Torquato, S.; Car, R. The phase diagram of high-pressure superionic ice. *Nat. Commun.* **2015**, *6* (1), 1−8.
(79) Millot, M.; Hamel, S.; Rygg, J. R.; Celliers, P. M.; Collins, G. W.; Coppari, F.; Fratanduono, D. E.; Jeanloz, R.; Swift, D. C.; Eggert, J. H. Experimental evidence for superionic water ice using shock compression. *Nat. Phys.* **2018**, *14* (3), 297−302.
(80) Kamaya, N.; Homma, K.; Yamakawa, Y.; Hirayama, M.; Kanno, R.; Yonemura, M.; Kamiyama, T.; Kato, Y.; Hama, S.; Kawamoto, K.; Mitsui, A. A lithium superionic conductor. *Nature materials* **2011**, *10* (9), 682−686.
(81) Bron, P.; Johansson, S.; Zick, K.; Schmedt auf der Günne, J.; Dehnen, S.; Roling, B. Li10SnP2S12: An Affordable Lithium Superionic Conductor. *J. Am. Chem. Soc.* **2013**, *135* (42), 15694−15697.
(82) Zhang, Z.; Shao, Y.; Lotsch, B.; Hu, Y.-S.; Li, H.; Janek, J.; Nazar, L. F.; Nan, C.-W.; Maier, J.; Armand, M.; Chen, L. New horizons for inorganic solid state ion conductors. *Energy Environ. Sci.* **2018**, *11* (8), 1945−1976.
(83) Zhang, H.; Wang, X.; Chremos, A.; Douglas, J. F. Superionic UO2: A model anharmonic crystalline material. *J. Chem. Phys.* **2019**, *150* (17), 174506.
(84) Stramare, S.; Thangadurai, V.; Weppner, W. Lithium Lanthanum Titanates: A Review. *Chem. Mater.* **2003**, *15* (21), 3974−3990.
(85) Knauth, P. Inorganic solid Li ion conductors: An overview. *Solid State Ionics* **2009**, *180* (14), 911−916.
(86) Thangadurai, V.; Narayanan, S.; Pinzaru, D. Garnet-type solid-state fast Li ion conductors for Li batteries: critical review. *Chem. Soc. Rev.* **2014**, *43* (13), 4714−4727.
(87) Bachman, J. C.; Muy, S.; Grimaud, A.; Chang, H.-H.; Pour, N.; Lux, S. F.; Paschos, O.; Maglia, F.; Lupart, S.; Lamp, P.; Giordano, L.; Shao-Horn, Y. Inorganic Solid-State Electrolytes for Lithium Batteries: Mechanisms and Properties Governing Ion Conduction. *Chem. Rev.* **2016**, *116* (1), 140−162.
(88) Chen, R.; Qu, W.; Guo, X.; Li, L.; Wu, F. The pursuit of solid-state electrolytes for lithium batteries: from comprehensive insight to emerging horizons. *Materials Horizons* **2016**, *3* (6), 487−516.
(89) He, X.; Zhu, Y.; Mo, Y. Origin of fast ion diffusion in super-ionic conductors. *Nat. Commun.* **2017**, *8* (1), 15893.
(90) Smith, J. G.; Siegel, D. J. Low-temperature paddlewheel effect in glassy solid electrolytes. *Nat. Commun.* **2020**, *11* (1), 1483.
(91) Wu, E. A.; Banerjee, S.; Tang, H.; Richardson, P. M.; Doux, J.-M.; Qi, J.; Zhu, Z.; Grenier, A.; Li, Y.; Zhao, E.; Deysher, G.; Sebti, E.; Nguyen, H.; Stephens, R.; Verbist, G.; Chapman, K. W.; Clément, R. J.; Banerjee, A.; Meng, Y. S.; Ong, S. P. A stable cathode-solid electrolyte composite for high-voltage, long-cycle-life solid-state sodium-ion batteries. *Nat. Commun.* **2021**, *12* (1), 1256.
(92) Horowitz, Y.; Lifshitz, M.; Greenbaum, A.; Feldman, Y.; Greenbaum, S.; Sokolov, A. P.; Golodnitsky, D. Review—Polymer/Ceramic Interface Barriers: The Fundamental Challenge for Advancing Composite Solid Electrolytes for Li-Ion Batteries. *J. Electrochem. Soc.* **2020**, *167* (16), 160514.
(93) Armand, M. The history of polymer electrolytes. *Solid State Ionics* **1994**, *69* (3), 309−319.
(94) Austen Angell, C.; Ansari, Y.; Zhao, Z. Ionic Liquids: Past, present and future. *Faraday Discuss.* **2012**, *154* (0), 9−27.
(95) Grundy, L. S.; Shah, D. B.; Nguyen, H. Q.; Diederichsen, K. M.; Celik, H.; DeSimone, J. M.; McCloskey, B. D.; Balsara, N. P. Impact of Frictional Interactions on Conductivity, Diffusion, and Transference Number in Ether- and Perfluoroether-Based Electrolytes. *J. Electrochem. Soc.* **2020**, *167* (12), 120540.
(96) Nürnberg, P.; Atik, J.; Borodin, O.; Winter, M.; Paillard, E.; Schönhoff, M. Superionicity in Ionic-Liquid-Based Electrolytes Induced by Positive Ion−Ion Correlations. *J. Am. Chem. Soc.* **2022**, *144* (10), 4657−4666.
(97) Zhang, H.; Wang, X.; Yu, H.-B.; Douglas, J. F. Dynamic heterogeneity, cooperative motion, and Johari−Goldstein $$\beta $$-relaxation in a metallic glass-forming material exhibiting a fragile-to-strong transition. *Eur. Phys. J. E* **2021**, *44* (4), 56.
(98) Zhang, H.; Wang, X.; Yu, H.-B.; Douglas, J. F. Fast dynamics in a model metallic glass-forming material. *J. Chem. Phys.* **2021**, *154* (8), 084505.
(99) Ise, N.; Yoshida, H. Paradoxes of the Repulsion-Only Assumption. *Acc. Chem. Res.* **1996**, *29* (1), 3−5.
(100) Wang, Y.; Fan, F.; Agapov, A. L.; Saito, T.; Yang, J.; Yu, X.; Hong, K.; Mays, J.; Sokolov, A. P. Examination of the fundamental relation between ionic transport and segmental relaxation in polymer electrolytes. *Polymer* **2014**, *55* (16), 4067−4076.
(101) Wang, Y.; Sun, C.-N.; Fan, F.; Sangoro, J. R.; Berman, M. B.; Greenbaum, S. G.; Zawodzinski, T. A.; Sokolov, A. P. Examination of methods to determine free-ion diffusivity and number density from analysis of electrode polarization. *Phys. Rev. E* **2013**, *87* (4), 042308.
(102) Chintapalli, M.; Timachova, K.; Olson, K. R.; Mecham, S. J.; Devaux, D.; DeSimone, J. M.; Balsara, N. P. Relationship between Conductivity, Ion Diffusion, and Transference Number in Perfluoropolyether Electrolytes. *Macromolecules* **2016**, *49* (9), 3508−3515.
(103) Mongcopa, K. I. S.; Gribble, D. A.; Loo, W. S.; Tyagi, M.; Mullin, S. A.; Balsara, N. P. Segmental Dynamics Measured by Quasi-Elastic Neutron Scattering and Ion Transport in Chemically Distinct Polymer Electrolytes. *Macromolecules* **2020**, *53* (7), 2406−2411.
(104) Bée, M. Localized and long-range diffusion in condensed matter: state of the art of QENS studies and future prospects. *Chem. Phys.* **2003**, *292* (2), 121−141.
(105) Lewis, R. M.; Jackson, G. L.; Maher, M. J.; Kim, K.; Narayanan, S.; Lodge, T. P.; Mahanthappa, M. K.; Bates, F. S. Grain Growth and Coarsening Dynamics in a Compositionally Asymmetric Block Copolymer Revealed by X-ray Photon Correlation Spectroscopy. *Macromolecules* **2020**, *53* (19), 8233−8243.
(106) Chen, Q.; Tudryn, G. J.; Colby, R. H. Ionomer dynamics and the sticky Rouse model. *J. Rheol.* **2013**, *57* (5), 1441−1462.

(107) Saalwächter, K., Multiple-Quantum NMR Studies of Anisotropic Polymer Chain Dynamics. In *Modern Magnetic Resonance*, Webb, G. A., Ed.; Springer International Publishing: Cham, 2017; pp 1−28.
(108) Saalwächter, K.; Herrero, B.; López-Manchado, M. A. Chain Order and Cross-Link Density of Elastomers As Investigated by Proton Multiple-Quantum NMR. *Macromolecules* **2005**, *38* (23), 9650−9660.
(109) Dudowicz, J.; Douglas, J. F.; Freed, K. F. The meaning of the "universal" WLF parameters of glass-forming polymer liquids. *J. Chem. Phys.* **2015**, *142* (1), 014905.
(110) Douglas, J. F. A dynamic measure of order in structural glasses. *Comput. Mater. Sci.* **1995**, *4* (4), 292−308.
(111) Mei, W.; Rothenberger, A. J.; Bostwick, J. E.; Rinehart, J. M.; Hickey, R. J.; Colby, R. H. Zwitterions Raise the Dielectric Constant of Soft Materials. *Phys. Rev. Lett.* **2021**, *127* (22), 228001.
(112) Ohno, H.; Yoshizawa-Fujita, M.; Kohno, Y. Design and properties of functional zwitterions derived from ionic liquids. *Phys. Chem. Chem. Phys.* **2018**, *20* (16), 10978−10991.
(113) Tiyapiboonchaiya, C.; Pringle, J. M.; Sun, J.; Byrne, N.; Howlett, P. C.; MacFarlane, D. R.; Forsyth, M. The zwitterion effect in high-conductivity polyelectrolyte materials. *Nat. Mater.* **2004**, *3* (1), 29−32.
(114) Zhang, W.; Richter, F. H.; Culver, S. P.; Leichtweiss, T.; Lozano, J. G.; Dietrich, C.; Bruce, P. G.; Zeier, W. G.; Janek, J. Degradation Mechanisms at the Li10GeP2S12/LiCoO2 Cathode Interface in an All-Solid-State Lithium-Ion Battery. *ACS Appl. Mater. Interfaces* **2018**, *10* (26), 22226−22236.
(115) Ning, Z.; Jolly, D. S.; Li, G.; De Meyere, R.; Pu, S. D.; Chen, Y.; Kasemchainan, J.; Ihli, J.; Gong, C.; Liu, B.; Melvin, D. L. R.; Bonnin, A.; Magdysyuk, O.; Adamson, P.; Hartley, G. O.; Monroe, C. W.; Marrow, T. J.; Bruce, P. G. Visualising Plating-Induced Cracking in Lithium Anode Solid Electrolyte Cells. *Nat. Mater.* **2021**, *20*, 1121−1129.
(116) Yuan, C.; Lu, W.; Xu, J. Unlocking the Electrochemical−Mechanical Coupling Behaviors of Dendrite Growth and Crack Propagation in All-Solid-State Batteries. *Adv. Energy Mater.* **2021**, *11* (36), 2101807.
(117) Cabana, J.; Kwon, B. J.; Hu, L. Mechanisms of degradation and strategies for the stabilization of cathode−electrolyte interfaces in Li-ion batteries. *Acc. Chem. Res.* **2018**, *51* (2), 299−308.
(118) Grady, Z. A.; Wilkinson, C. J.; Randall, C. A.; Mauro, J. C., Emerging Role of Non-crystalline Electrolytes in Solid-State Battery Research. *Frontiers in Energy Research* **2020**, *8*, DOI: 10.3389/fenrg.2020.00218.
(119) Jones, S. D.; Nguyen, H.; Richardson, P. M.; Chen, Y.-Q.; Wyckoff, K. E.; Hawker, C. J.; Clément, R. J.; Fredrickson, G. H.; Segalman, R. A. Design of Polymeric Zwitterionic Solid Electrolytes with Superionic Lithium Transport. *ACS Central Science* **2022**, *8* (2), 169−175.
(120) Jones, S. D.; Chen, Y.-Q.; Richardson, P. M.; Hawker, C. J.; Clemente, R. J.; Fredrickson, G. H.; Segalman, R. A. *Design of Polymeric Zwitterionic Lithium Conductors − Impact of Tethered Ion Identity, in press.*
(121) Yoshizawa, M.; Narita, A.; Ohno, H. Design of Ionic Liquids for Electrochemical Applications. *Aust. J. Chem.* **2004**, *57* (2), 139−144.
(122) Makhlooghiazad, F.; O'Dell, L. A.; Porcarelli, L.; Forsyth, C.; Quazi, N.; Asadi, M.; Hutt, O.; Mecerreyes, D.; Forsyth, M.; Pringle, J. M. Zwitterionic materials with disorder and plasticity and their application as non-volatile solid or liquid electrolytes. *Nat. Mater.* **2022**, *21* (2), 228−236.
(123) Narita, A.; Shibayama, W.; Ohno, H. Structural factors to improve physico-chemical properties of zwitterions as ion conductive matrices. *J. Mater. Chem.* **2006**, *16* (15), 1475−1482.
(124) Abbott, L. J.; Lawson, J. W. Effects of Side Chain Length on Ionic Aggregation and Dynamics in Polymer Single-Ion Conductors. *Macromolecules* **2019**, *52* (19), 7456−7467.
(125) Ono, A.; Ohno, H.; Kato, T.; Ichikawa, T. Design of 3D continuous proton conduction pathway by controlling co-organization behavior of gemini amphiphilic zwitterions and acids. *Solid State Ionics* **2018**, *317*, 39−45.
(126) Ichikawa, T.; Yoshio, M.; Hamasaki, A.; Taguchi, S.; Liu, F.; Zeng, X.-B.; Ungar, G.; Ohno, H.; Kato, T. Induction of Thermotropic Bicontinuous Cubic Phases in Liquid-Crystalline Ammonium and Phosphonium Salts. *J. Am. Chem. Soc.* **2012**, *134* (5), 2634−2643.
(127) Ichikawa, T.; Kato, T.; Ohno, H. 3D Continuous Water Nanosheet as a Gyroid Minimal Surface Formed by Bicontinuous Cubic Liquid-Crystalline Zwitterions. *J. Am. Chem. Soc.* **2012**, *134* (28), 11354−11357.
(128) Galizia, M.; Chi, W. S.; Smith, Z. P.; Merkel, T. C.; Baker, R. W.; Freeman, B. D. 50th Anniversary Perspective: Polymers and Mixed Matrix Membranes for Gas and Vapor Separation: A Review and Prospective Opportunities. *Macromolecules* **2017**, *50* (20), 7809−7843.
(129) Comesaña-Gándara, B.; Chen, J.; Bezzu, C. G.; Carta, M.; Rose, I.; Ferrari, M.-C.; Esposito, E.; Fuoco, A.; Jansen, J. C.; McKeown, N. B. Redefining the Robeson upper bounds for CO2/CH4 and CO2/N2 separations using a series of ultrapermeable benzotriptycene-based polymers of intrinsic microporosity. *Energy Environ. Sci.* **2019**, *12* (9), 2733−2740.
(130) Wang, Y.; Agapov, A. L.; Fan, F.; Hong, K.; Yu, X.; Mays, J.; Sokolov, A. P. Decoupling of Ionic Transport from Segmental Relaxation in Polymer Electrolytes. *Phys. Rev. Lett.* **2012**, *108* (8), 088303.
(131) Okumura, T.; Nishimura, S. Lithium ion conductive properties of aliphatic polycarbonate. *Solid State Ionics* **2014**, *267*, 68−73.
(132) Van Humbeck, J. F.; Aubrey, M. L.; Alsbaiee, A.; Ameloot, R.; Coates, G. W.; Dichtel, W. R.; Long, J. R. Tetraarylborate polymer networks as single-ion conducting solid electrolytes. *Chemical Science* **2015**, *6* (10), 5499−5505.
(133) Ji, Y.; Yang, K.; Liu, M.; Chen, S.; Liu, X.; Yang, B.; Wang, Z.; Huang, W.; Song, Z.; Xue, S.; Fu, Y.; Yang, L.; Miller, T. S.; Pan, F. PIM-1 as a Multifunctional Framework to Enable High-Performance Solid-State Lithium−Sulfur Batteries. *Adv. Funct. Mater.* **2021**, *31* (47), 2104830.
(134) Mitsuda, H.; Uno, T.; Kubo, M.; Itoh, T. Solid Polymer Electrolytes Based on Poly(1,3-diacetyl-4-imidazolin-2-one). *Polym. Bull.* **2006**, *57* (3), 313−319.
(135) Marken, F.; Carta, M.; McKeown, N. B. Polymers of Intrinsic Microporosity in the Design of Electrochemical Multicomponent and Multiphase Interfaces. *Anal. Chem.* **2021**, *93* (3), 1213−1220.
(136) He, Y.; Qiao, Y.; Chang, Z.; Zhou, H. The potential of electrolyte filled MOF membranes as ionic sieves in rechargeable batteries. *Energy Environ. Sci.* **2019**, *12* (8), 2327−2344.
(137) Moon, J. D.; Bridge, A. T.; D'Ambra, C.; Freeman, B. D.; Paul, D. R. Gas separation properties of polybenzimidazole/thermally-rearranged polymer blends. *J. Membr. Sci.* **2019**, *582*, 182−193.
(138) Luo, S.; Stevens, K. A.; Park, J. S.; Moon, J. D.; Liu, Q.; Freeman, B. D.; Guo, R. Highly CO2-Selective Gas Separation Membranes Based on Segmented Copolymers of Poly(Ethylene oxide) Reinforced with Pentiptycene-Containing Polyimide Hard Segments. *ACS Appl. Mater. Interfaces* **2016**, *8* (3), 2306−2317.
(139) Stoeva, Z.; Martin-Litas, I.; Staunton, E.; Andreev, Y. G.; Bruce, P. G. Ionic Conductivity in the Crystalline Polymer Electrolytes PEO6:LiXF6, X = P, As, Sb. *J. Am. Chem. Soc.* **2003**, *125* (15), 4619−4626.
(140) Nakamura, T.; Akutagawa, T.; Honda, K.; Underhill, A. E.; Coomber, A. T.; Friend, R. H. A molecular metal with ion-conducting channels. *Nature* **1998**, *394* (6689), 159−162.
(141) Moriya, M.; Kato, D.; Hayakawa, Y.; Sakamoto, W.; Yogo, T. Crystal structure and solid state ionic conductivity of molecular crystal composed of lithium bis(trifluoromethanesulfonyl)amide and 1,2-dimethoxybenzene in a 1:1 molar ratio. *Solid State Ionics* **2016**, *285*, 29−32.

(142) Moriya, M.; Kitaguchi, H.; Nishibori, E.; Sawa, H.; Sakamoto, W.; Yogo, T. Molecular Ionics in Supramolecular Assemblies with Channel Structures Containing Lithium Ions. *Chemistry − A European Journal* **2012**, *18* (48), 15305−15309.
(143) Sanders, R. A.; Frech, R.; Khan, M. A. Structural Investigation of Crystalline and Solution Phases in N,N,N′,N′-Tetramethylethylenediamine (TMEDA) with Lithium Triflate (LiCF3SO3) and Sodium Triflate (NaCF3SO3). *J. Phys. Chem. B* **2003**, *107* (33), 8310−8315.
(144) Liu, J.; Upadhyay, S.; Schaefer, J. Improved conductivity of single-component, ion-condensed smectic liquid crystalline electrolytes. *ChemRxiv Materials Science May 27*, 2022, DOI: 10.26434/chemrxiv-2022-crzzq (accessed September 1, 2022).
(145) Jackson, G. L.; Perroni, D. V.; Mahanthappa, M. K. Roles of Chemical Functionality and Pore Curvature in the Design of Nanoporous Proton Conductors. *J. Phys. Chem. B* **2017**, *121* (40), 9429−9436.
(146) Yang, X. H.; Tan, S.; Liang, T.; Wei, B. Z.; Wu, Y. A unidomain membrane prepared from liquid-crystalline poly(pyridinium 4-styrene sulfonate) for anhydrous proton conduction. *J. Membr. Sci.* **2017**, *523*, 355−360.
(147) Xie, W. T.; Tan, S.; Yang, J.; Luo, J.; Wang, C. H.; Wu, Y. Ionic Liquid Crystalline Composite Membranes Composed of Smectic Imidazolium Hydrogen Sulfate and Polyvinyl Alcohol for Anhydrous Proton Conduction. *Ind. Eng. Chem. Res.* **2020**, *59* (18), 8632−8639.
(148) Xie, W.; Tan, S.; Yang, J.; Luo, J.; Wang, C.; Wu, Y. Ionic Liquid Crystalline Composite Membranes Composed of Smectic Imidazolium Hydrogen Sulfate and Polyvinyl Alcohol for Anhydrous Proton Conduction. *Ind. Eng. Chem. Res.* **2020**, *59* (18), 8632−8639.
(149) Yang, X.; Tan, S.; Liang, T.; Wei, B.; Wu, Y. A unidomain membrane prepared from liquid-crystalline poly(pyridinium 4-styrene sulfonate) for anhydrous proton conduction. *J. Membr. Sci.* **2017**, *523*, 355−360.
(150) Siddiqui, J. A.; Wright, P. V. Electroactive films from poly(ethylene oxide)-sodium iodide complexes with tetracyanoquinodimethan. *Faraday Discuss. Chem. Soc.* **1989**, *88* (0), 113−122.
(151) Wang, Y.; Zanelotti, C. J.; Wang, X. E.; Kerr, R.; Jin, L. Y.; Kan, W. H.; Dingemans, T. J.; Forsyth, M.; Madsen, L. A. Solid-state rigid-rod polymer composite electrolytes with nanocrystalline lithium ion pathways. *Nat. Mater.* **2021**, *20* (9), 1255.
(152) Dias, F. B.; Voss, J. P.; Batty, S. V.; Wright, P. V.; Ungar, G. Smectic phases in a novel alkyl-substituted polyether and its complex with lithium tetrafluoroborate. *Macromol. Rapid Commun.* **1994**, *15* (12), 961−969.
(153) Patel, J. P.; Wright, P. V.; Dunmur, D. A.; Tajbakhsh, A. R. Isomorphous mixing of mesogenic anions and uncharged analogues in organised poly(ehtylene oxide)-alkali salt complexes. *Adv. Mater. Opt. Electron.* **1994**, *4* (4), 265−271.
(154) McHattie, G. S.; Imrie, C. T.; Ingram, M. D. Ionically conducting side chain liquid crystal polymer electrolytes. *Electrochim. Acta* **1998**, *43* (10), 1151−1154.
(155) Imrie, C. T.; Ingram, M. D.; McHattie, G. S. Ion Transport in Glassy Side-Group Liquid Crystalline Polymer Electrolytes. *Adv. Mater.* **1999**, *11* (10), 832−834.
(156) Imrie, C. T.; Ingram, M. D.; McHattie, G. S. Ion Transport in Glassy Polymer Electrolytes. *J. Phys. Chem. B* **1999**, *103* (20), 4132−4138.
(157) Hall, L. M.; Seitz, M. E.; Winey, K. I.; Opper, K. L.; Wagener, K. B.; Stevens, M. J.; Frischknecht, A. L. Ionic Aggregate Structure in Ionomer Melts: Effect of Molecular Architecture on Aggregates and the Ionomer Peak. *J. Am. Chem. Soc.* **2012**, *134* (1), 574−587.
(158) Hall, L. M.; Stevens, M. J.; Frischknecht, A. L. Dynamics of Model Ionomer Melts of Various Architectures. *Macromolecules* **2012**, *45* (19), 8097−8108.
(159) Bolintineanu, D. S.; Stevens, M. J.; Frischknecht, A. L. Influence of Cation Type on Ionic Aggregates in Precise Ionomers. *Macromolecules* **2013**, *46* (13), 5381−5392.
(160) Bolintineanu, D. S.; Stevens, M. J.; Frischknecht, A. L. Atomistic Simulations Predict a Surprising Variety of Morphologies in Precise Ionomers. *ACS Macro Lett.* **2013**, *2* (3), 206−210.
(161) Buitrago, C. F.; Bolintineanu, D. S.; Seitz, M. E.; Opper, K. L.; Wagener, K. B.; Stevens, M. J.; Frischknecht, A. L.; Winey, K. I. Direct Comparisons of X-ray Scattering and Atomistic Molecular Dynamics Simulations for Precise Acid Copolymers and Ionomers. *Macromolecules* **2015**, *48* (4), 1210−1220.
(162) Evans, C. M.; Bridges, C. R.; Sanoja, G. E.; Bartels, J.; Segalman, R. A. Role of Tethered Ion Placement on Polymerized Ionic Liquid Structure and Conductivity: Pendant versus Backbone Charge Placement. *ACS Macro Lett.* **2016**, *5* (8), 925−930.
(163) Kuray, P.; Noda, T.; Matsumoto, A.; Iacob, C.; Inoue, T.; Hickner, M. A.; Runt, J. Ion Transport in Pendant and Backbone Polymerized Ionic Liquids. *Macromolecules* **2019**, *52* (17), 6438−6448.
(164) Yan, L.; Rank, C.; Mecking, S.; Winey, K. I. Gyroid and Other Ordered Morphologies in Single-Ion Conducting Polymers and Their Impact on Ion Conductivity. *J. Am. Chem. Soc.* **2020**, *142* (2), 857−866.
(165) Buitrago, C. F.; Opper, K. L.; Wagener, K. B.; Winey, K. I. Precise Acid Copolymer Exhibits a Face-Centered Cubic Structure. *ACS Macro Lett.* **2012**, *1* (1), 71−74.
(166) Buitrago, C. F.; Alam, T. M.; Opper, K. L.; Aitken, B. S.; Wagener, K. B.; Winey, K. I. Morphological Trends in Precise Acid- and Ion-Containing Polyethylenes at Elevated Temperature. *Macromolecules* **2013**, *46* (22), 8995−9002.
(167) Buitrago, C. F.; Jenkins, J. E.; Opper, K. L.; Aitken, B. S.; Wagener, K. B.; Alam, T. M.; Winey, K. I. Room Temperature Morphologies of Precise Acid- and Ion-Containing Polyethylenes. *Macromolecules* **2013**, *46* (22), 9003−9012.
(168) Abbott, L. J.; Buss, H. G.; Thelen, J. L.; McCloskey, B. D.; Lawson, J. W. Polyanion Electrolytes with Well-Ordered Ionic Layers in Simulations and Experiment. *Macromolecules* **2019**, *52* (15), 5518−5528.
(169) Paren, B. A.; Nguyen, N.; Ballance, V.; Hallinan, D. T.; Kennemur, J. G.; Winey, K. I. Superionic Li-Ion Transport in a Single-Ion Conducting Polymer Blend Electrolyte. *Macromolecules* **2022**, *55* (11), 4692−4702.
(170) Zheng, Y.; Chia, F.; Ungar, G.; Wright, P. V. Self-tracking in solvent-free, low-dimensional polymer electrolyte blends with lithium salts giving high ambient DC conductivity. *Chem. Commun.* **2000**, No. 16, 1459−1460.
(171) Zheng, Y.; Chia, F.; Ungar, G.; Richardson, T. H.; Wright, P. V. High ambient dc and ac conductivities in solvent-free, low-dimensional polymer electrolyte blends with lithium salts. *Electrochim. Acta* **2001**, *46* (10), 1397−1405.
(172) Zheng, Y.; Wright, P. V.; Ungar, G. Insertion of ionophobic components into amphiphilic low-dimensional polymer electrolytes. *Electrochim. Acta* **2000**, *45* (8), 1161−1165.
(173) You, C.; Wu, X.; Yuan, X.; Chen, Y.; Liu, L.; Zhu, Y.; Fu, L.; Wu, Y.; Guo, Y.-G.; van Ree, T. Advances in rechargeable Mg batteries. *Journal of Materials Chemistry A* **2020**, *8* (48), 25601−25625.
(174) Wang, N.; Wan, H.; Duan, J.; Wang, X.; Tao, L.; Zhang, J.; Wang, H. A review of zinc-based battery from alkaline to acid. *Materials Today Advances* **2021**, *11*, 100149.
(175) Tu, J.; Song, W.-L.; Lei, H.; Yu, Z.; Chen, L.-L.; Wang, M.; Jiao, S. Nonaqueous Rechargeable Aluminum Batteries: Progresses, Challenges, and Perspectives. *Chem. Rev.* **2021**, *121* (8), 4903−4961.
(176) Schauser, N. S.; Seshadri, R.; Segalman, R. A. Multivalent ion conduction in solid polymer systems. *Molecular Systems Design & Engineering* **2019**, *4* (2), 263−279.
(177) Kas'yanova, A. V.; Lyagaeva, Y. G.; Danilov, N. A.; Plaksin, S. V.; Farlenkov, A. S.; Medvedev, D. A.; Demin, A. K. Ceramic and Transport Characteristics of Electrolytes Based on Mg-Doped LaYO3. *Russian Journal of Applied Chemistry* **2018**, *91* (5), 770−777.
(178) Kim, H. S.; Arthur, T. S.; Allred, G. D.; Zajicek, J.; Newman, J. G.; Rodnyansky, A. E.; Oliver, A. G.; Boggess, W. C.; Muldoon, J.

Structure and compatibility of a magnesium electrolyte with a sulphur cathode. *Nat. Commun.* **2011**, *2* (1), 427.
(179) Kim, S. S.; Bevilacqua, S. C.; See, K. A. Conditioning-Free Mg Electrolyte by the Minor Addition of Mg(HMDS)2. *ACS Appl. Mater. Interfaces* **2020**, *12* (5), 5226−5233.
(180) Roy, S.; Thirumoorthy, K.; Padidela, U. K.; Vairaprakash, P.; Anoop, A.; Thimmakondu, V. S. Organomagnesium Crown Ethers and Their Binding Affinities with Li+, Na+, K+, Be2+, Mg2+, and Ca2+ Ions − A Theoretical Study. *ChemistrySelect* **2021**, *6* (33), 8782−8790.
(181) Shi, J.; Vincent, C. A. The effect of molecular weight on cation mobility in polymer electrolytes. *Solid State Ionics* **1993**, *60* (1), 11−17.
(182) Vincent, C. A. Ion transport in polymer electrolytes. *Electrochim. Acta* **1995**, *40* (13), 2035−2040.
(183) Marchiori, C. F. N.; Carvalho, R. P.; Ebadi, M.; Brandell, D.; Araujo, C. M. Understanding the Electrochemical Stability Window of Polymer Electrolytes in Solid-State Batteries from Atomic-Scale Modeling: The Role of Li-Ion Salts. *Chem. Mater.* **2020**, *32* (17), 7237−7246.
(184) Méry, A.; Rousselot, S.; Lepage, D.; Dollé, M. A Critical Review for an Accurate Electrochemical Stability Window Measurement of Solid Polymer and Composite Electrolytes. *Materials (Basel)* **2021**, *14* (14), 3840.
(185) Usiskin, R.; Maier, J. Interfacial Effects in Lithium and Sodium Batteries. *Adv. Energy Mater.* **2021**, *11* (2), 2001455.
(186) Wang, A.; Kadam, S.; Li, H.; Shi, S.; Qi, Y. Review on modeling of the anode solid electrolyte interphase (SEI) for lithium-ion batteries. *npj Computational Materials* **2018**, *4* (1), 15.

https://doi.org/10.1021/acspolymersau.2c00024
ACS Polym. Au 2022, 2, 430−448